

# Sequential Membership Inference Attacks

Thomas Michel<sup>1</sup> Debabrota Basu<sup>1</sup> Emilie Kaufmann<sup>1</sup>

## Abstract

Modern AI models are not static. They go through multiple updates in their lifecycles. Thus, exploiting the model dynamics to create stronger Membership Inference (MI) attacks and tighter privacy audits are timely questions. Though the literature empirically shows that using a sequence of model updates can increase the power of MI attacks, rigorous analysis of the ‘optimal’ MI attacks is limited to static models with infinite samples. Hence, we develop an ‘optimal’ MI attack, SeMI\*, that uses the sequence of model updates to *identify the presence of a target inserted at a certain update step*. For the empirical mean computation, we derive the optimal power of SeMI\*, while accessing a finite number of samples with or without privacy. Our results retrieve the existing asymptotic analysis. We observe that having access to the model sequence avoids the dilution of MI signals unlike the existing attacks on the final model, where the MI signal vanishes as training data accumulates. Furthermore, an adversary can use SeMI\* to tune both the insertion time and the canary to yield tighter privacy audits. Finally, we conduct experiments across data distributions and models trained or fine-tuned with DP-SGD demonstrating that practical variants of SeMI\* lead to tighter privacy audits than the baselines.

## 1. Introduction

Machine Learning (ML) models memorize training data, creating privacy risks for individuals whose data were used to develop them (Shokri et al., 2017; Carlini et al., 2022a). Privacy auditing quantifies these risks by testing whether specific records can be detected in the training set. Membership Inference (MI) attacks serve as the primary tool for auditing: an attacker who distinguishes members from non-members with high confidence establishes an empirical

<sup>1</sup>Univ. Lille, Inria, CNRS, Centrale Lille, UMR 9189-CRISStAL, France. Correspondence to: Thomas Michel <thomas.michel@inria.fr>.

lower bound on the model’s privacy leakage (Jayaraman & Evans, 2019; Jagielski et al., 2020; Nasr et al., 2023). Audits with higher distinguishing power yield tighter bounds.

Privacy auditing has been developed to complement differential privacy (Dwork et al., 2006; Dwork & Roth, 2014). Early work establishes that even simple statistical models leak membership information (Homer et al., 2008). Theoretical analysis shows that privacy depends on the ratio of dimensionality to sample size (Sankararaman et al., 2009). Jayaraman & Evans (2019) found 5–10× gaps between theoretical DP guarantees and empirical privacy estimates. Techniques for tight auditing (Nasr et al., 2023; Steinke et al., 2023) and debugging (Tramer et al., 2022) close this gap by crafting adversarial targets and observing model updates during training. *Our approach shows how exploiting intermediate observations can yield tighter privacy audits.*

Specifically, standard auditing practice targets a specific snapshot of a model. The auditor selects a target point (a.k.a. canary), queries the model, and applies a membership test. Target selection matters: points ‘far’ from the data distribution leak more information than typical points (Azize & Basu, 2025; Carlini et al., 2022b). *Modern ML models are dynamic: they rarely exist as isolated snapshots.* Continuous training updates the deployed models as new data arrives. Fine-tuning adapts the base models to specific tasks. Federated learning aggregates updates from different users across rounds. *In each case, multiple model versions become accessible*, whether through public release, API versioning, or checkpoint access during training.

Jagielski et al. (2023) demonstrate that combining the MI scores across model updates improves attack accuracy. They apply standard MI attacks separately to each model snapshot, and then, aggregate the scores via difference or ratio operations. Related work on model updates includes reconstruction attacks (Salem et al., 2020) that recover data from online learning updates, machine unlearning attacks (Chen et al., 2020), and leakage analysis of snapshots in NLP (Zanella-Béguin et al., 2020). *Our approach differs by deriving the optimal test via likelihood ratio analysis and identifying the insertion time of a canary as a new actionable lever for tighter audits.*

*We study Membership Inference (MI) when the auditor observes a sequence of  $T$  model snapshots rather than a single*

static one. The sequential setting offers two levers for designing tight audits: *selecting targets that leak information, and choosing when to insert them*. Specifically, we ask:

1. *Are there advantages of the MI tests accessing a sequence of models in comparison to a static test on the final model?*
2. *Does the knowledge of the insertion time affect the power of sequential MI tests?*
3. *Can sequential MI tests lead to theoretically and practically tighter privacy audits?*

**Our contributions** address these questions affirmatively.

**(1) Optimal MI test with sequential access.** Motivated by the optimal MI attack for the static setting (Azize & Basu, 2025) derived from the Neyman-Pearson lemma (Neyman & Pearson, 1933), we derive the optimal MI attack in the sequential setting, which is a sequential likelihood ratio test crafted with an insertion time. We refer to it as SeMI\*. Specifically, for the empirical mean computation from Gaussian data, we derive a closed-form analysis of the sequential MI attack.

**(2) Isolation property of sequential MI test.** We further observe a unique phenomenon for the sequential MI test on the empirical mean, namely *isolation property*. This means that consecutive outputs reveal the batch mean at insertion time  $\tau$  exactly. The likelihood ratio depends only on this recovered batch statistic. Rather than detecting the target among all cumulative samples, the sequential test operates on an isolated batch of size  $n$ . For the empirical mean under stationary conditions, test power depends only on batch size and target distance from the mean, not on  $\tau$  or  $T$ . By contrast, a single-observation test applied to the final output must detect the target among  $nT$  samples; its influence diminishes as training data accumulates. Sequential observation eliminates this dilution.

**(3) Adapting MI tests with the insertion time.** As insertion time emerges as a unique lever for sequential MI tests, we study the impact of the knowledge of the insertion time. We study three likelihood ratio based tests, SeMI\*, SeMI<sub>unif</sub> and SeMI<sub>max</sub>, that respectively assume  $\tau$  is known, uniformly distributed, or can be anything. We derive their powers for the empirical mean mechanism. Our numerical studies show that SeMI\* achieves the best power while the other two behave similarly.

**(4) Extending sequential MI tests to Gradient Descent (GD).** Since GD-type algorithms (Kiefer & Wolfowitz, 1952) and their variants are the standard to train modern ML models, we further extend the design of sequential MI tests to Stochastic GD (SGD) and DP-SGD (Abadi et al., 2016) for batch training, namely SeMI<sub>SGD</sub>. We clarify the practical relaxations needed to extend the sequential MI tests to the practical ML models. Our numerical studies for SGD and DP-SGD show similar improvements achieved by

the sequential MI test and impact of the insertion time as in the empirical mean setting.

**(5) From tighter sequential MI tests to sequential privacy audits.** First, we formalize sequential privacy auditing as a hypothesis testing game that encodes the auditor's control over target selection and insertion time. We test the proposed sequential privacy audit with SeMI for private fine-tuning of models with DP-SGD. Experimental results across datasets, models, and pre-defined privacy levels illustrate that SeMI<sub>SGD</sub> generally exhibits tighter privacy audits than the baselines, especially in the high privacy regimes.

## 2. Auditing and Membership Inference for Sequential Mechanisms

We assume data is sequentially collected over  $T$  steps. At each step  $t \in \{1, \dots, T\}$ , a fresh batch of data  $D_t$  consisting of  $n$  samples arrives. Each sample is drawn i.i.d. from a distribution  $\mathcal{D}_t$ . At step  $t$ , a sequential mechanism  $\mathcal{M}_t$  is applied to the accumulated dataset, releasing output  $o_t \triangleq \mathcal{M}_t\left(\bigcup_{i=1}^t D_i\right)$ . We let  $\mathcal{M}$  denote the composed global mechanism whose input is the joint dataset  $D \triangleq \bigcup_{i=1}^T D_i$  and output is the whole sequence  $o \triangleq (o_1, \dots, o_T)$  obtained via the intermediate mechanisms  $\mathcal{M}_1, \dots, \mathcal{M}_T$ . This formalism models an ML system which is retrained as new data arrives, and each version is released or accessible to users. The mechanisms and distributions may vary over time. We are interested in assessing the privacy level achieved by the global mechanism  $\mathcal{M}$ , while having access to the intermediate mechanisms  $\mathcal{M}_1, \dots, \mathcal{M}_T$ .

To quantify the privacy level of a mechanism, we adhere to the classical  $(\varepsilon, \delta)$ -Differential Privacy (DP) framework (Dwork & Roth, 2014).  $\mathcal{M}$  satisfies  $(\varepsilon, \delta)$ -DP if for all measurable sets of output  $S$  and datasets  $D, D'$  differing in one element, and some  $\varepsilon > 0$  and  $\delta \in [0, 1)$ ,

$$\Pr[\mathcal{M}(D) \in S] \leq e^\varepsilon \Pr[\mathcal{M}(D') \in S] + \delta. \quad (1)$$

Given some  $\delta$ , privacy auditing amounts to finding a lower bound on  $\varepsilon$  for which the inequality (1) is satisfied.

There are two dominant approaches to auditing. The first is to estimate the maximum  $\varepsilon$  for which  $\max\{\Pr[\mathcal{M}(D) \in S] - e^\varepsilon \Pr[\mathcal{M}(D') \in S], 0\}$ , known as the *hockey-stick* divergence, is less than  $\delta$  (Koskela & Mohammadi, 2024; Basu & Chanda, 2026). The second is to leverage the hypothesis testing interpretation of DP (Wasserman & Zhou, 2010; Kairouz et al., 2015) that conducts MI tests and uses the error probabilities of the tests to create a lower bound on  $\varepsilon$ . As the second approach additionally provides insights for designing optimal MI tests and the most privacy leaking canaries (Nasr et al., 2023; Azize & Basu, 2025), we explore it for the sequential mechanisms.

**Algorithm 1** Crafter with Insertion Time Control

---

```

1: Input: Mechanisms  $(\mathcal{M}_1, \dots, \mathcal{M}_T)$ , data distributions
    $(\mathcal{D}_1, \dots, \mathcal{D}_T)$ , batch size  $n$ , target  $z^*$ , distributions  $\nu_B$ ,
   distribution  $\nu_\tau$ 
2: Sample  $B \sim \nu_B$  and  $\tau \sim \nu_\tau$ 
3: for  $t = 1, \dots, T$  do
4:   Sample batch  $D_t \sim \mathcal{D}_t^n$ 
5:   if  $B = 1$  and  $t = \tau$  then
6:     Sample  $j \sim \text{Uniform}(\{1, \dots, n\})$ 
7:     Replace  $D_t[j] \leftarrow z^*$ 
8:   end if
9:   Compute  $o_t = \mathcal{M}_t \left( \bigcup_{i=1}^t D_i \right)$ 
10: end for
11: Output:  $(o_1, \dots, o_T), B, \tau$ 

```

---

**MI tests** are binary hypothesis tests that try to identify whether a particular target  $z^*$  is present in the input dataset  $D$  by observing the output of a mechanism (Carlini et al., 2022a; Ye et al., 2022; Leemann et al., 2023). Furthermore, a crafter is deployed to design a canary  $z^*$ , and then, to decide whether to insert  $z^*$  in the dataset or not.

In the sequential model access setting, we further ask whether  $z^*$  belongs to a specific sub-dataset  $D_\tau$ , where  $\tau \in \mathbb{N}$  denotes the insertion time. Specifically, as we observe the model updates one by one, a sequential MI test works with two hypothesis classes parameterized by  $z^*$ :

**H<sub>0</sub> (OUT)** :  $D \sim \mathcal{P}_0$ , if for all  $t \in [T]$ ,  $D_t \sim \mathcal{D}_t^{\otimes n}$ .

**H<sub>1</sub> (IN)** :  $D \sim \mathcal{P}_1^\tau$ , if for all  $t \in [T]$ ,  $D_t \sim \mathcal{D}_t^{\otimes n}$ , and then given  $J \sim \mathcal{U}([n])$ , the  $J$ -th entry of  $D_\tau$  is replaced by  $z^*$ .

We define a probability model parameterized by  $\nu_B$ , i.e., a distribution over  $\{0, 1\}$ , and  $\nu_\tau$ , i.e., a distribution over  $\{1, \dots, T\}$ . Under this model, we draw an insertion indicator  $B \sim \nu_B$  and an insertion time  $\tau \sim \nu_\tau$ . If  $B = 0$ , we draw  $D \sim \mathcal{P}_0$ . If  $B = 1$ , we draw  $D \sim \mathcal{P}_1^\tau$ . The mechanism  $\mathcal{M}$  produces output  $(o_1, \dots, o_T)$ . A sequential MI test  $\mathcal{A}$  maps the output sequence to a prediction  $\hat{B} = \mathcal{A}_{z^*, \tau}(o_1, \dots, o_T)$ , where the subscript indicates that the test depends on the target  $z^*$  and the insertion time  $\tau$ . Algorithm 2 formalizes the **Sequential Membership Inference (SeMI)** game used to estimate these error rates, whereas Algorithm 1 demonstrates a crafter that leverages a distribution  $\nu_\tau$  over insertion time to choose the exact step  $\tau$ , where it inserts the canary in the dataset.

**Lemma 2.1** (Connecting MI Test Error and Privacy Audits (Kairouz et al., 2015)). *Let  $\alpha(\mathcal{A}) \triangleq \mathbb{P}(\hat{B} = 1 | B = 0)$  and  $\beta(\mathcal{A}) \triangleq \mathbb{P}(\hat{B} = 0 | B = 1)$  be the Type I and Type II errors of an MI test  $\mathcal{A}$ , respectively. If the mechanism  $\mathcal{M}$  is  $(\varepsilon, \delta)$ -DP, the following holds for any MI test*

$$\alpha(\mathcal{A}) + e^\varepsilon \beta(\mathcal{A}) \geq 1 - \delta, \quad \beta(\mathcal{A}) + e^\varepsilon \alpha(\mathcal{A}) \geq 1 - \delta.$$

Consequently, any MI test  $\mathcal{A}$  provides the following lower

**Algorithm 2** Sequential MI Game (SeMI)

---

```

1: Input: Mechanisms  $(\mathcal{M}_1, \dots, \mathcal{M}_T)$ , data distributions
    $(\mathcal{D}_1, \dots, \mathcal{D}_T)$ , batch size  $n$ , target  $z^*$ , distribution  $\nu_\tau$ ,
   adversary  $\mathcal{A}_{z^*, \tau}$ , rounds  $R$ 
2: for  $r = 1, \dots, R$  do
3:    $(o_1, \dots, o_T), B_r, \tau \leftarrow \text{Crafter}((\mathcal{M}_t), (\mathcal{D}_t), n, z^*)$ 
4:    $\hat{B}_r \sim \mathcal{A}_{z^*, \tau}(o_1, \dots, o_T)$ 
5: end for
6: Output:  $B, \hat{B}$ 

```

---

bound on  $\varepsilon$ :

$$\varepsilon \geq \log \left( \max \left[ \frac{1 - \delta - \alpha(\mathcal{A})}{\beta(\mathcal{A})}, \frac{1 - \delta - \beta(\mathcal{A})}{\alpha(\mathcal{A})} \right] \right). \quad (2)$$

A practical lower bound further requires upper bounds on  $\alpha(\mathcal{A})$  and  $\beta(\mathcal{A})$  that can be obtained from multiple executions of the MI test (i.e. from the output of Algorithm 2). In Section 5, we provide a concrete instantiation of these error upper bounds for MI tests that threshold some test statistic, as well as the resulting high-probability lower bound on  $\varepsilon$ .

To obtain a tight lower bound, we seek to design a crafter and a sequential MI test (often called an adversary in auditing literature) that together achieve least possible  $\alpha$  and  $\beta$ , i.e. maximum accuracy in SeMI game.

The connection to statistical hypothesis testing guides the design of effective adversaries. Here, we consider the white-box setting (Sablayrolles et al., 2019; Carlini et al., 2022a; Nasr et al., 2023; Maddock et al., 2023), where the adversary observes the sequence of data distributions  $(\mathcal{D}_t)$  and mechanisms  $(\mathcal{M}_t)$ , batch size  $n$ , and total steps  $T$ .

When  $\tau$  is also known, computing  $\hat{B}$  is a test of

$$\mathbf{H}_0 \text{ (OUT)} : (D \sim \mathcal{P}_0) \text{ against } \mathbf{H}_\tau \text{ (IN}_\tau\text{)} : (D \sim \mathcal{P}_1^\tau) \quad (3)$$

based on observing  $(o_1, \dots, o_T)$ . When  $\tau$  is unknown to the adversary, so that  $\hat{B} = \mathcal{A}_{z^*}(o_1, \dots, o_T)$ , the test becomes

$$\widetilde{\mathbf{H}}_0 \text{ (OUT)} : (D \sim \mathcal{P}_0) \text{ against } \widetilde{\mathbf{H}}_1 \text{ (IN)} : (D \sim \widetilde{\mathcal{P}}_1), \quad (4)$$

where  $\widetilde{\mathcal{P}}_1$  is defined as  $\tau \sim \nu_\tau$  and then  $D | \tau \sim \mathcal{P}_1^\tau$ .

When the data-generating distributions  $\mathcal{D}_1, \dots, \mathcal{D}_T$  are known, both the problems reduce to testing simple hypotheses, for which the Neyman-Pearson lemma (Neyman & Pearson, 1933) establishes Likelihood Ratio (LR) tests to be optimal. Since the SeMI provides sequential access of the mechanisms, the question is: *How to use the sequence of input-output data to compute a sequence of LR statistics and combine them over time to design efficient SeMI tests?*

In the next sections, we design multiple SeMI tests that lead to tighter bounds on  $\varepsilon$  than the optimal MI test having access to only the final model.

### 3. Sequential Membership Inference

For theoretical rigor, we commence with the empirical mean mechanism of Gaussian data and derive the closed-form expressions of three SeMI tests: one knowing the insertion time, one assuming it be uniformly random and one considering the worst case. We show that knowing  $\tau$  yields the most powerful SeMI test, SeMI\*, which is also significantly better than having access to only the final model.

#### 3.1. Optimal Test: SeMI\*

We analyze the empirical mean mechanism  $\mathcal{M}^{\text{emp}}$  in a stationary setting, where  $\mathcal{D}_t = \mathcal{D} = \mathcal{N}(\mu, \Sigma)$  for all  $t$ , with mean vector  $\mu \in \mathbb{R}^d$  and a positive definite covariance matrix  $\Sigma \in \mathbb{R}^{d \times d}$ . Each batch  $D_t$  contains  $n$  i.i.d. samples from  $\mathcal{D}_t$ .<sup>1</sup> At step  $t$ , the mechanism outputs an empirical estimate of the cumulative mean  $\hat{\mu}_t \triangleq \frac{1}{nt} \sum_{j=1}^t \sum_{k=1}^n \mathbf{X}_{j,k}$  that satisfies the recursion  $\hat{\mu}_t = (1 - \frac{1}{t})\hat{\mu}_{t-1} + \frac{1}{t}\bar{\mathbf{X}}_t$ , where  $\bar{\mathbf{X}}_t \triangleq \frac{1}{n} \sum_{k=1}^n X_{t,k}$  is the batch mean.

**Theorem 3.1** (Multivariate Log Likelihood Ratio (LR)). *Let  $\mathbf{N}_\tau \triangleq \bar{\mathbf{X}}_\tau - \mu$ . The log-LR for testing  $\mathbf{H}_0$  against  $\mathbf{H}_1^\tau$  is*

$$\begin{aligned} \log \text{LR}_\tau = & -\frac{d}{2} \log \left( \frac{n-1}{n} \right) - \frac{n}{2(n-1)} \mathbf{N}_\tau^\top \Sigma^{-1} \mathbf{N}_\tau \\ & + \frac{n}{n-1} \mathbf{N}_\tau^\top \Sigma^{-1} (\mathbf{z}^* - \mu) - \frac{m^*}{2(n-1)}, \end{aligned} \quad (5)$$

where  $m^* = (\mathbf{z}^* - \mu)^\top \Sigma^{-1} (\mathbf{z}^* - \mu)$  is the squared Mahalanobis distance of the target from the population mean.

**Connection to the Asymptotic Results.** The test statistic depends on the target through its Mahalanobis distance  $m^*$ , i.e., targets farther from the population mean in the metric induced by  $\Sigma^{-1}$  are more detectable. This parallels the asymptotic analysis of [Aize & Basu \(2025\)](#) showing that MI power scales with the Mahalanobis distance when both  $d$  and  $n \rightarrow \infty$  and  $\frac{d}{n} = \mathcal{O}(1)$ . Our result provides the exact finite-sample likelihood ratio that yields an additional quadratic term in  $\mathbf{N}_\tau$ . This term becomes negligible as  $n \rightarrow \infty$  and we retrieve their test statistic.

We refer to the test comparing the test statistic of Equation (5) to some threshold  $\gamma$  as SeMI\*. Appendix B provides the full derivation and error analysis. The cornerstone of the proof of Theorem 3.1 is the following simplification of the likelihood ratio.

**Lemma 3.2.** *The likelihood ratio for testing  $\mathbf{H}_0$  against  $\mathbf{H}_1^\tau$  based on  $(\hat{\mu}_1, \dots, \hat{\mu}_T)$  satisfies*

$$\frac{p(\hat{\mu}_1, \dots, \hat{\mu}_T \mid \mathbf{H}_1^\tau)}{p(\hat{\mu}_1, \dots, \hat{\mu}_T \mid \mathbf{H}_0)} = \frac{p(\hat{\mu}_\tau \mid \hat{\mu}_{\tau-1}, \mathbf{H}_1^\tau)}{p(\hat{\mu}_\tau \mid \hat{\mu}_{\tau-1}, \mathbf{H}_0)}.$$

<sup>1</sup>Though we analyse for a fixed batch size, SeMI can tackle varying batch sizes.

The full likelihood ratio factorizes as a product of conditional densities over all transitions. For  $t \neq \tau$ , the conditional distribution of  $\hat{\mu}_t$  given  $\hat{\mu}_{t-1}$  is identical under both hypotheses because the target  $z^*$  either has not yet been inserted ( $t < \tau$ ) or its effect is absorbed into  $\hat{\mu}_{t-1}$  ( $t > \tau$ ). These terms cancel leaving only the transition at time  $\tau$ .

**Derivation of Power of SeMI\*.** Now, to explain the isolation property and compare the power of the test with that on the final model, we focus on the univariate case ( $d = 1$ ). With  $\mathcal{D} = \mathcal{N}(\mu, \sigma^2)$ , the empirical mean mechanism outputs  $\hat{\mu}_t = \frac{1}{nt} \sum_{j=1}^t \sum_{k=1}^n X_{j,k}$ . Thus, the conditional distributions of empirical means at insertion time  $\tau$  are

$$\begin{aligned} \hat{\mu}_\tau \mid \hat{\mu}_{\tau-1}, \mathbf{H}_0 & \sim \mathcal{N} \left( \frac{\tau-1}{\tau} \hat{\mu}_{\tau-1} + \frac{\mu}{\tau}, \frac{\sigma^2}{\tau^2 n} \right) \\ \hat{\mu}_\tau \mid \hat{\mu}_{\tau-1}, \mathbf{H}_1^\tau & \sim \mathcal{N} \left( \frac{\tau-1}{\tau} \hat{\mu}_{\tau-1} + \frac{(n-1)\mu + z^*}{\tau n}, \right. \\ & \quad \left. \frac{(n-1)\sigma^2}{\tau^2 n^2} \right) \end{aligned}$$

Under  $\mathbf{H}_1^\tau$ , the mean shifts by  $(z^* - \mu)/(\tau n)$  and the variance decreases by a factor of  $(n-1)/n$  since one sample is fixed rather than random.

**Remark 3.3 (Isolation Property).** We observe that given consecutive observations  $(\hat{\mu}_{\tau-1}, \hat{\mu}_\tau)$ , the batch mean can be exactly recovered, i.e.,  $\bar{X}_\tau = \tau \hat{\mu}_\tau - (\tau-1) \hat{\mu}_{\tau-1}$ . Thus, the likelihood ratio depends on the data only through  $\bar{X}_\tau$ . Since it is independent of the batches before and after, and also  $T$ , we refer to it as the isolation property of SeMI\*.

**Theorem 3.4** (Log Likelihood Ratio). *The log likelihood ratio for univariate samples has the form*

$$\begin{aligned} \log \text{LR}_\tau = & -\frac{1}{2} \log \left( \frac{n-1}{n} \right) - \frac{n}{2(n-1)\sigma^2} (\bar{X}_\tau - \mu)^2 \\ & + \frac{(z^* - \mu)n}{(n-1)\sigma^2} (\bar{X}_\tau - \mu) - \frac{(z^* - \mu)^2}{2(n-1)\sigma^2}. \end{aligned}$$

The test statistic is quadratic in the deviation  $\bar{X}_\tau - \mu$ . The linear term captures alignment between the batch mean and the target direction, while the negative quadratic term penalizes large deviations from the population mean. The constant terms depend only on the signal strength  $(z^* - \mu)/\sigma$  and the batch size  $n$ .

**Lemma 3.5** (Type I Error). *Define  $\gamma_{\max} = \frac{1}{2} \left[ \frac{(z^* - \mu)^2}{\sigma^2} - \log \left( \frac{n-1}{n} \right) \right]$ . For  $\gamma > \gamma_{\max}$ , we have  $\alpha(\gamma) = 0$ . For  $\gamma \leq \gamma_{\max}$ :*

$$\alpha(\gamma) = \Phi(a + b(\gamma)) - \Phi(a - b(\gamma))$$

where  $m^* = \frac{(z^* - \mu)^2}{\sigma^2}$ ,  $a = \sqrt{m^* n}$  and  $b(\gamma) = \sqrt{(n-1)(m^* - \log(1 - \frac{1}{n}) - 2\gamma)}$ .

**Lemma 3.6** (Type II Error). *For  $\gamma \leq \gamma_{\max}$ , with  $a$  and  $b(\gamma)$  as defined above:*

$$\begin{aligned}\beta(\gamma) &= \Phi \left( a \sqrt{\frac{n-1}{n}} - b(\gamma) \sqrt{\frac{n}{n-1}} \right) \\ &+ \Phi \left( -a \sqrt{\frac{n-1}{n}} - b(\gamma) \sqrt{\frac{n}{n-1}} \right)\end{aligned}$$

Both errors depend on the batch size  $n$  and the signal strength  $(z^* - \mu)^2 / \sigma^2$  indicating  $z^*$ 's membership but not on the insertion time  $\tau$  or the number of batches  $T$ . This  $\tau$ -invariance follows from the isolation property, i.e., the test operates on the recovered batch mean  $\bar{X}_\tau$ , which has the same distribution regardless of when the insertion occurred.

**Comparison with the Final Observation Test.** When only the final output  $\hat{\mu}_T$  is observed, the test statistic has the same form, but with  $n$  replaced by  $nT$ . We call this baseline the *Final Observation* test.

**Lemma 3.7** (Final Observation Type I Error). *For the Final Observation test with  $\gamma_{\max}^{(T)} = \frac{1}{2} \left[ \frac{(z^* - \mu)^2}{\sigma^2} - \log \left( \frac{nT-1}{nT} \right) \right]$  and  $\gamma \leq \gamma_{\max}^{(T)}$ , the Type I error*

$$\begin{aligned}\alpha_{FO}(\gamma) &= \Phi(a_T + b_T(\gamma)) - \Phi(a_T - b_T(\gamma)) \\ \text{where } a_T &= \sqrt{m^* nT} \quad \text{and} \quad b_T(\gamma) = \\ &\sqrt{(nT-1) \left( m^* - \log \left( 1 - \frac{1}{nT} \right) - 2\gamma \right)}.\end{aligned}$$

**Lemma 3.8** (Final Observation Type II Error). *For  $\gamma \leq \gamma_{\max}^{(T)}$ , with  $a_T$  and  $b_T(\gamma)$  as defined above, the Type II error*

$$\begin{aligned}\beta_{FO}(\gamma) &= \Phi \left( a_T \sqrt{\frac{nT-1}{nT}} - b_T(\gamma) \sqrt{\frac{nT}{nT-1}} \right) \\ &+ \Phi \left( -a_T \sqrt{\frac{nT-1}{nT}} - b_T(\gamma) \sqrt{\frac{nT}{nT-1}} \right).\end{aligned}$$

SeMI\* operates on a batch of size  $n$ , while Final Observation test must detect the target among  $nT$  samples. As  $T$  increases, the target's signal  $(z^* - \mu)/(nT)$  vanishes for Final Observation, while SeMI\* retains constant power.

*Remark 3.9* (Adapting to Distribution Shifts). The analysis of SeMI\* extends to the non-stationary setting, where  $D_t \sim \mathcal{N}(\mu_t, \sigma_t^2)$ . The likelihood ratio depends only on  $(\mu_\tau, \sigma_\tau^2)$ , while for  $t \neq \tau$ , conditioning on  $\hat{\mu}_{t-1}$  yields identical distributions under both hypotheses. The extension with time-varying parameters is given in Appendix C.

### 3.2. Adapting SeMI with Insertion Times

We now ask: *what is the best possible MI test that is agnostic to  $\tau$ ?* This models an adversary who knows that the target  $z_*$  may have been inserted but does not know when.

As discussed in Section 2, such an MI test can be obtained from a statistical test in which the alternative is  $\mathbf{H}_1$ :  $\tau$  is drawn from  $\nu_\tau$  (the distribution used by Crafter) and then the dataset is generated from  $\mathcal{P}_1^\tau$ . Since both  $\mathbf{H}_0$  and  $\mathbf{H}_1$  specify complete distributions over the observations, the Neyman-Pearson lemma also applies, i.e., the optimal test thresholds the likelihood ratio.

**Optimal test for uniform  $\tau$ .** For  $\nu_\tau \triangleq \mathcal{U}(\{1, \dots, T\})$ , we give the expression of the likelihood ratio,  $\text{LR}_{\text{Unif}}$ . We call SeMI<sup>Unif</sup> the test that thresholds  $\log \text{LR}_{\text{Unif}}$ .

**Theorem 3.10** (Uniform  $\tau$  Likelihood Ratio). *Let  $\text{LR}_t$  be the likelihood ratio for  $\mathbf{H}_0$  against  $\mathbf{H}_1^t$  from Theorem 3.1. The likelihood ratio for testing  $\mathbf{H}_0$  against  $\widetilde{\mathbf{H}}_1$  is*

$$\text{LR}_{\text{Unif}} = \frac{1}{T} \sum_{t=1}^T \text{LR}_t.$$

The marginal likelihood under  $\widetilde{\mathbf{H}}_1$  is obtained by averaging over  $\tau$ , i.e., conditioned on  $\tau = t$ , the data distribution matches  $\mathbf{H}_1^t$ , so the marginal is  $(1/T) \sum_t P(\text{data} \mid \mathbf{H}_1^t)$ . Dividing by the null likelihood yields the arithmetic mean of individual likelihood ratios. Details in Appendix D.

**Relation to a GLR test.** Using that  $\max_t \text{LR}_t \leq \sum_{t=1}^T \text{LR}_t \leq T \max_t \text{LR}_t$  yields

$$\max_t \log \text{LR}_t - \log T \leq \log \text{LR}_{\text{Unif}} \leq \max_t \log \text{LR}_t.$$

This shows that SeMI<sup>Unif</sup> is quite close to the test that uses  $\max_t \log \text{LR}_t$  as a test statistic. We call it SeMI<sup>max</sup>. Interestingly, SeMI<sup>max</sup> can be interpreted as a Generalized Likelihood Ratio test (Zeitouni et al., 2002; Van Trees, 2004) of  $\mathbf{H}_0$  against  $\bigcup_t \mathbf{H}_1^t$ . This is a composite hypothesis testing problem and there are no optimality guarantees for the resulting GLR test, but its connexion to SeMI<sup>Unif</sup> suggests that it can also lead to a good MI test.

In Section 3.3, we observe from experimental results that SeMI<sup>Unif</sup> and SeMI<sup>max</sup> have comparable performance, and they are both outperformed by SeMI\*. We further conjecture that replacing the uniform distribution by another distribution would lead to comparable performance.

### 3.3. Numerical Analysis: Sequential Advantage

The theoretical analysis identifies three aspects of the sequential advantage, i.e. accessing the sequence of models rather than only the final one.

First, *isolation*: SeMI\* produces a discrete jump in the test statistic at  $\tau$  with stable separation thereafter.

Second, *power*: SeMI\* achieves higher power than Final Observation at all false positive rates, with the gap widening as the target's Mahalanobis distance increases.

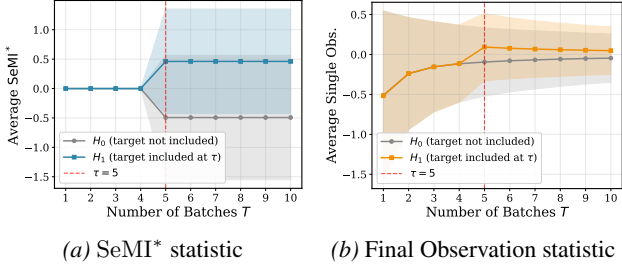


Figure 1. Log-likelihood ratio statistics as a function of observed updates ( $n = 10, \tau = 5$ ). (a) SeMI\*: separation appears at  $\tau$  and remains constant. (b) Final Observation: separation appears at  $\tau$  but decreases as  $T$  grows.

Third, *scaling with  $T$* : SeMI\* power remains constant as  $T$  increases (since it depends only on batch size  $n$ ), while Final Observation power degrades (since the target's influence diminishes among  $nT$  samples).

We illustrate these properties using the Gaussian empirical mean mechanism. We sample  $T = 10$  batches of size  $n = 10$  from  $\mathcal{N}(0, 1)$ . The target  $z^* = 3$  (Mahalanobis distance 3 from the distribution) is inserted at  $\tau = 5$ .

Figure 1 tracks the log-likelihood ratio for a target inserted at  $\tau = 5$ . The SeMI\* statistic exhibits a sharp, sustained step at  $\tau$ , effectively isolating the signal. In contrast, the Final Observation statistic shows a smaller jump that diminishes as  $T$  grows, illustrating how the signal dilutes over time.

Figure 2 compares SeMI\* (known  $\tau$ ) against SeMI<sup>Unif</sup>, SeMI<sup>max</sup>, and Final Observation. As predicted, SeMI\* maintains constant power regardless of  $T$ , confirming the isolation property. While SeMI<sup>Unif</sup> and SeMI<sup>max</sup> degrade with  $T$ , they consistently outperform Final Observation, especially for targets far from the distribution mean (high Mahalanobis distance). The errors are estimated using  $R = 50,000$  runs of SeMI with  $\nu_\tau = \delta_{\{\tau\}}$  in the Crafter. Similar results are obtained for  $\nu_\tau = \mathcal{U}([T])$ . ROC curves and results under uniformly sampled  $\tau$  appear in Appendix H.1, displaying very similar dynamics to the fixed  $\tau$  case. Appendix H.3 shows that test power depends on the Mahalanobis distance rather than the data dimension  $d$ .

## 4. Sequential MI for Gradient Descent

The empirical mean analysis establishes the sequential advantage in an idealized setting. To audit real ML models, we need tests that apply to gradient descent, the algorithm used to train virtually all modern models. Prior sequential attacks on SGD rely on heuristic score combinations (Jagielinski et al., 2023). A principled likelihood ratio test for SGD would enable tighter privacy audits by exploiting the same isolation property that benefits the empirical mean.

We observe model parameters  $\theta_0, \theta_1, \dots, \theta_T$  with  $\theta_t \in \mathbb{R}^d$ . At each step  $t$ , the update is  $\theta_t = \theta_{t-1} - \eta_t g_t$  where  $\eta_t > 0$

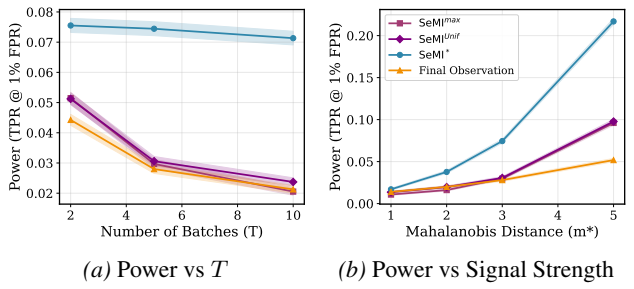


Figure 2. Comparison of sequential tests ( $n = 10, z^*$  with Mahalanobis distance 3). (a) Power (TPR at 1% FPR) vs number of updates  $T$ . (b) Power vs target Mahalanobis distance ( $T = 5$ ).

is the learning rate and  $g_t = \frac{1}{n_t} \sum_{x \in D_t} \nabla_\theta \ell(\theta_{t-1}; x)$  is the batch gradient on dataset  $D_t$  of size  $n_t$ . As in Section 3, we test  $\mathbf{H}_0$  (target  $z^*$  not in the training data) against  $\mathbf{H}_1^*$  (target inserted in batch  $D_\tau$ ).

### 4.1. Sequential Test for SGD

We assume that, conditioned on  $\theta_{t-1}$ , the batch gradient  $g_t$  is Gaussian with mean  $\mu_g(\theta_{t-1})$  and covariance  $\Sigma_g(\theta_{t-1})/n_t$ . This approximation can be justified by the central limit theorem when the batch aggregates gradients from many data points.

Under this assumption, the conditional distributions mirror the empirical mean case. Under  $\mathbf{H}_0$ : for all  $t$ ,

$$\theta_t \mid \theta_{t-1}, \mathbf{H}_0 \sim \mathcal{N} \left( \theta_{t-1} - \eta_t \mu_g(\theta_{t-1}), \frac{\eta_t^2 \Sigma_g(\theta_{t-1})}{n_t} \right).$$

Under  $\mathbf{H}_1^*$  with one sample in  $D_\tau$  replaced by target  $z^*$ :

$$\theta_\tau \mid \theta_{\tau-1}, \mathbf{H}_1^* \sim \mathcal{N} \left( \theta_{\tau-1} - \eta_\tau \frac{(n_\tau - 1)\mu_g + g^*}{n_\tau}, \frac{\eta_\tau^2 (n_\tau - 1)\Sigma_g}{n_\tau^2} \right)$$

where  $g^* = \nabla_\theta \ell(\theta_{\tau-1}; z^*)$  is the target gradient, and we write  $\mu_g$  and  $\Sigma_g$  for  $\mu_g(\theta_{\tau-1})$  and  $\Sigma_g(\theta_{\tau-1})$ .

The likelihood ratio factorizes as in Lemma 3.2: only the transition at time  $\tau$  contributes.

**Theorem 4.1** (SeMI<sup>SGD</sup> Log Likelihood Ratio). *Define  $\delta_g = \nabla_\theta \ell(\theta_{\tau-1}; z^*) - \mu_g(\theta_{\tau-1})$  and  $N = \theta_\tau - \theta_{\tau-1} + \eta_\tau \mu_g(\theta_{\tau-1})$ . The log likelihood ratio is:*

$$\begin{aligned} \log \text{LR} = & -\frac{d}{2} \log \left( \frac{n_\tau - 1}{n_\tau} \right) - \frac{n_\tau}{2(n_\tau - 1)\eta_\tau^2} N^\top \Sigma_g^{-1} N \\ & - \frac{n_\tau}{(n_\tau - 1)\eta_\tau} N^\top \Sigma_g^{-1} \delta_g - \frac{m^*}{2(n_\tau - 1)} \end{aligned}$$

where  $m^* = \delta_g^\top \Sigma_g^{-1} \delta_g$  is the Mahalanobis distance of the target gradient from the population mean.

The test statistic  $\text{SeMI}^{\text{SGD}}$  has the same structure as Theorem 3.1, with the batch mean replaced by the scaled parameter update  $N/\eta_\tau$ .  $\delta_g$  measures how much the target's gradient deviates from the population mean of the gradient: targets whose gradients differ substantially from typical gradients are more detectable. The Mahalanobis distance  $m^*$  accounts for the gradient covariance structure, giving less weight to directions with high variance.

**Isolation Property for SGD.** From consecutive parameter observations  $(\theta_{\tau-1}, \theta_\tau)$ , the scaled update  $N$  can be computed exactly. The likelihood ratio depends only on this quantity, not on earlier or later parameters. This mirrors the isolation property for the empirical mean.

**Numerical Analysis: Linear Regression.** Unlike the empirical mean setting, where the population statistics are fixed, SGD introduces a complication: the gradient mean  $\mu_g(\theta)$  and covariance  $\Sigma_g(\theta)$  vary with the model parameters. This variation means that a target may be easier to detect at certain stages of training than others, depending on how the test statistic evolves along the optimization trajectory. Experiments on linear regression with Gaussian data confirm that  $\text{SeMI}^{\text{SGD}}$  achieves higher power than heuristic baselines, and that insertion time affects power, although differently depending on the method (Appendix H.2). Section 5 extends this comparison to privacy auditing on real datasets.

## 4.2. Practical Extensions

In order to practically use  $\text{SeMI}^{\text{SGD}}$  for privacy audits of neural networks, we need to first adapt it to the private variant of SGD, called DP-SGD (Abadi et al., 2016), and estimate three quantities: the population mean gradient  $\mu_g(\theta_{\tau-1})$ , the gradient covariance  $\Sigma_g(\theta_{\tau-1})$ , and the target gradient  $\nabla_\theta \ell(\theta_{\tau-1}; z^*)$ .

**Application to DP-SGD.** For differentially private training via DP-SGD, each update includes clipped gradients and Gaussian noise:  $\theta_t = \theta_{t-1} - \eta_t(g_t^{\text{clip}} + \xi_t)$  where  $\xi_t \sim \mathcal{N}(0, \sigma_{\text{DP}}^2 C^2 I/n_t^2)$  with clipping threshold  $C$ . The noise reduces test power but preserves the sequential structure and the isolation property. Section 5 applies  $\text{SeMI}^{\text{SGD}}$  to privacy auditing of DP-SGD fine-tuning on real datasets.

**Estimation with Reference Data.** Since, in practice, the three quantities of interest in Theorem 4.1 are not known, the adversary estimates  $\mu_g$  and  $\Sigma_g$  from reference data drawn from the same distribution  $\mathcal{D}$ . Given  $m$  reference samples  $\{x_1, \dots, x_m\}$ , we compute  $\hat{\mu}_g = \frac{1}{m} \sum_{i=1}^m \nabla_\theta \ell(\theta_{\tau-1}; x_i)$ , and  $\hat{\Sigma}_g = \frac{1}{m-1} \sum_{i=1}^m (\nabla_\theta \ell(\theta_{\tau-1}; x_i) - \hat{\mu}_g)(\nabla_\theta \ell(\theta_{\tau-1}; x_i) - \hat{\mu}_g)^\top$ . The target gradient  $\nabla_\theta \ell(\theta_{\tau-1}; z^*)$  is computed directly from the target  $z^*$  and the observed parameter  $\theta_{\tau-1}$ .

## 5. Sequential Privacy Audits with SeMI

The empirical mean experiments (Section 3) establish the sequential advantage of  $\text{SeMI}^*$  in an idealized setting. Here, we test whether this advantage yields a tighter audit of real ML models. Hence, we use  $\text{SeMI}^{\text{SGD}}$  for privacy auditing of DP-SGD.

### 5.1. A High-probability Lower Bound on $\varepsilon$

$\text{SeMI}^*$  and all the competitors that we consider in this section are of the form  $\mathcal{A}_{z^*, \tau}^\gamma(o_1, \dots, o_T) = \mathbb{1}(T > \gamma)$  where  $T = T(o_1, \dots, o_T, \tau)$  is some test statistic and  $\gamma$  is some threshold. We now explain how to obtain a statistically valid lower bound on  $\varepsilon$  for an MI test of this form.

We run  $R$  rounds of SeMI game (Algorithm 2) and record the membership indicators  $B_1, \dots, B_R$  and the values of the test statistic  $T_1, \dots, T_R$  instead of the decision of test  $\hat{B}_1^\gamma, \dots, \hat{B}_R^\gamma$  for a particular choice of  $\gamma$ . Using the membership indicators and test statistics across the multiple runs, we can estimate the Type-I error  $\alpha(\gamma) = \alpha(\mathcal{A}_{z^*, \tau}^\gamma)$  and Type-II error  $\beta(\gamma) = \beta(\mathcal{A}_{z^*, \tau}^\gamma)$  of the MI test for any given threshold  $\gamma \in \mathbb{R}$  as  $\hat{\alpha}_R(\gamma) = \frac{1}{N_0(R)} \sum_{r=1}^R \mathbb{1}(T_r > \gamma) \mathbb{1}(B_r = 0)$  and  $\hat{\beta}_R(\gamma) = \frac{1}{N_1(R)} \sum_{r=1}^R \mathbb{1}(T_r \leq \gamma) \mathbb{1}(B_r = 1)$ . Here,  $N_i(R) = \sum_{r=1}^R \mathbb{1}(B_r = i)$  (for  $i \in \{0, 1\}$ ) denotes the number of times the MI test signals positive and negative memberships. Given  $\xi > 0$ , we introduce two upper confidence bounds on the errors

$$\begin{aligned} \bar{\alpha}_R^\xi(\gamma) &= \hat{\alpha}_R(\gamma) + \sqrt{\frac{\log(\xi/4)}{2N_0(R)}}, \\ \bar{\beta}_R^\xi(\gamma) &= \hat{\beta}_R(\gamma) + \sqrt{\frac{\log(\xi/4)}{2N_1(R)}}, \end{aligned}$$

and define

$$\underline{\varepsilon}_R^\xi(\delta) = \log \left( \max_{\gamma \in \mathbb{R}} \max \left[ \frac{1 - \delta - \bar{\alpha}_R^\xi(\gamma)}{\bar{\beta}_R^\xi(\gamma)}, \frac{1 - \delta - \bar{\beta}_R^\xi(\gamma)}{\bar{\alpha}_R^\xi(\gamma)} \right] \right).$$

**Lemma 5.1.** *If the mechanism used in SeMI satisfies  $(\varepsilon, \delta)$ -DP, then  $\mathbb{P}(\varepsilon \geq \underline{\varepsilon}_R^\xi(\delta)) \geq 1 - \xi$ .*

The proof, given in Appendix G, relies on uniform concentration of the empirical CDF of the test statistic, which allows to optimize over  $\gamma$ . Previous approaches (Nasr et al., 2021) instead built confidence bounds on the errors for each  $\gamma$  separately and then optimize over  $\gamma$ , which actually affects the overall statistical accuracy as it requires some union bound on  $\gamma$ .

### 5.2. Experiments: Auditing Private Fine-tuning

**Experimental Setup.** Models are pretrained on a public data split with SGD, then fine-tuned on a private split with

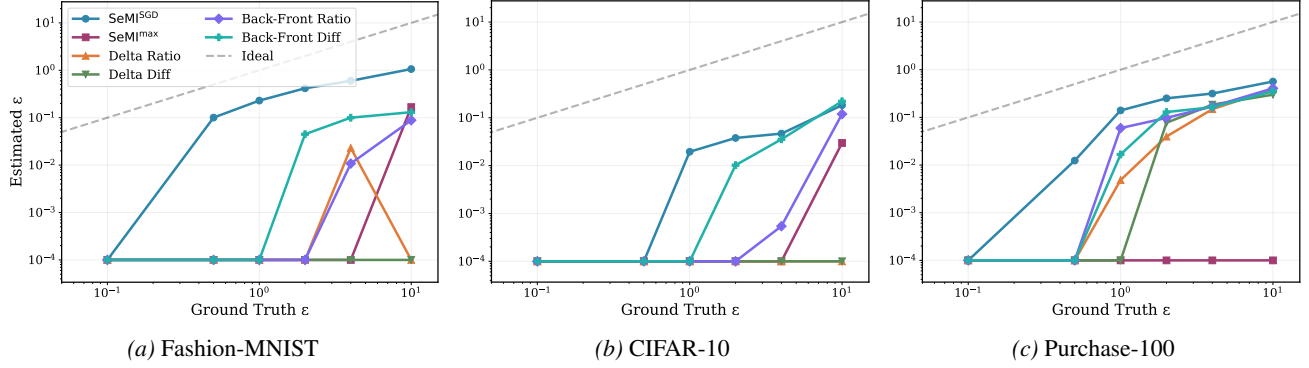


Figure 3. Privacy auditing of DP-SGD fine-tuning. Estimated  $\varepsilon$  (lower bound) versus ground truth  $\varepsilon$  for different attacks, averaged over insertion times  $\tau \in \{1, \dots, T\}$ . Closer to the diagonal (ideal) is better.  $\text{SeMI}^{\text{SGD}}$  yields tighter lower bounds than heuristic baselines.

DP-SGD (Abadi et al., 2016). We use batch size 64,  $T = 10$  updates, and  $\delta = 10^{-4}$ . The auditor observes the full parameter trajectory  $(\theta_0, \dots, \theta_T)$  and knows the insertion time  $\tau$ . For each audit, the target  $z^*$  is selected from a candidate pool by choosing the sample with highest gradient Mahalanobis distance, estimated from a held-out reference set. We average results over  $\tau \in \{1, \dots, T\}$  to assess performance across insertion times; Appendix H.5 shows that selecting the best  $\tau$  post hoc yields tighter bounds, though how to choose  $\tau$  a priori for a given architecture remains an open question.

**Datasets and Models.** We test three model architectures: multinomial logistic regression on Fashion-MNIST (Xiao et al., 2017), a frozen pretrained VGG-16 (Simonyan & Zisserman, 2014) with a single trainable layer on CIFAR-10 (Krizhevsky et al., 2009), and a fully connected network (128 hidden units) on Purchase-100 (Shokri et al., 2017).

**Hypothesis.** The likelihood ratio test  $\text{SeMI}^{\text{SGD}}$  with known insertion time  $\tau$  yields tighter privacy lower bounds than heuristic sequential attacks, because it exploits the isolation property to focus on the batch where the target was inserted.

**Baselines.** We compare against four heuristic attacks from (Jagielski et al., 2023). *Delta* attacks measure the maximum change in loss across consecutive updates. Delta Diff uses  $S = \max_t (\ell(\theta_{t-1}; z^*) - \ell(\theta_t; z^*))$  and Delta Ratio uses  $S = \max_t \ell(\theta_{t-1}; z^*) / \ell(\theta_t; z^*)$ . The *Back-Front* attacks measure the total change from initial to final model. Back-Front Diff uses  $S = \ell(\theta_0; z^*) - \ell(\theta_T; z^*)$  and Back-Front Ratio uses  $S = \ell(\theta_0; z^*) / \ell(\theta_T; z^*)$ . All baselines use loss values rather than gradients and are oblivious to  $\tau$ .

**Results.** Figure 3 shows  $\varepsilon_{\text{est}}$  versus ground truth  $\varepsilon$  across three datasets. On Fashion-MNIST, the hypothesis is supported:  $\text{SeMI}^{\text{SGD}}$  yields tighter privacy lower bounds than all baselines across the privacy range. On CIFAR-10 and Purchase-100,  $\text{SeMI}^{\text{SGD}}$  performs as well as or better than baselines, with the clearest gains in low-privacy regimes.

ROC curves in Appendix H.4 show that  $\text{SeMI}^{\text{SGD}}$  achieves near-perfect discrimination without DP noise and maintains an advantage at low false positive rates under DP-SGD. Appendix H.5 shows that selecting the best fixed insertion time can improve the tightness of the audit compared to averaging over  $\tau$ .

## 6. Discussion and Future Works

We derived the optimal membership inference test for sequential model observations and characterized its power in closed form for Gaussian data under the empirical mean mechanism. The isolation property shows that sequential access recovers the batch statistic at insertion time, eliminating the dilution effect that weakens static tests as training data accumulates. We designed tests for three insertion time scenarios: known, uniformly random, and unknown. The extension to SGD relies on batch gradient Gaussianity. Despite this strong assumption, experiments on DP-SGD fine-tuning show that  $\text{SeMI}^{\text{SGD}}$  yields tighter privacy lower bounds than heuristic baselines, with the strongest gains in low-privacy regimes.

An important aspect of model updates is distribution shift. Though we have shown that  $\text{SeMI}^*$  is robust to distribution shifts, it would be important to quantify the impact of distribution shift when the insertion time is unknown and chosen from a distribution by the Crafter. It is also interesting to study whether a Crafter can choose a distribution of insertion time that avoids detection by a privacy-preserving mechanism. Finally, like most of the tight privacy auditing literature, our audits of SGD and DP-SGD are white-box while the  $\text{SeMI}$  framework can generalize to black-box settings, i.e., when we do not have access to the gradients and can only query the models at each step to obtain the corresponding outputs. It will be interesting and practically useful to extend the optimal sequential MI tests and develop tight auditing mechanisms to the black-box setting.

## Acknowledgements

This work has been partially supported by the French National Research Agency (ANR) in the framework of the PEPR IA FOUNDRY project (ANR-23-PEIA-0003). We also acknowledge the Inria-ISI, Kolkata Associate Team “SeRAI”, and the ANR JCJC for the REPUBLIC project (ANR-22-CE23-0003-01) for partially supporting the project

## References

Abadi, M., Chu, A., Goodfellow, I., McMahan, H. B., Mironov, I., Talwar, K., and Zhang, L. Deep learning with differential privacy. In *Proceedings of the 2016 ACM SIGSAC conference on computer and communications security*, pp. 308–318, 2016.

Azize, A. and Basu, D. Some Targets Are Harder to Identify than Others: Quantifying the Target-dependent Membership Leakage, March 2025.

Basu, D. and Chanda, D. Sublinear algorithms for estimating wasserstein and TV distances: Applications to fairness and privacy auditing. *Transactions on Machine Learning Research*, 2026. ISSN 2835-8856. URL <https://openreview.net/forum?id=m26nTK1pCr>.

Carlini, N., Chien, S., Nasr, M., Song, S., Terzis, A., and Tramer, F. Membership inference attacks from first principles. In *2022 IEEE symposium on security and privacy (SP)*, pp. 1897–1914. IEEE, 2022a.

Carlini, N., Jagielski, M., Zhang, C., Papernot, N., Terzis, A., and Tramer, F. The privacy onion effect: Memorization is relative. *Advances in Neural Information Processing Systems*, 35:13263–13276, 2022b.

Chen, M., Zhang, Z., Wang, T., Backes, M., Humbert, M., and Zhang, Y. When machine unlearning jeopardizes privacy. *arXiv preprint arXiv:2005.02205*, 2020.

Dwork, C. and Roth, A. The algorithmic foundations of differential privacy. *Foundations and Trends in Theoretical Computer Science*, 9(3–4):211–407, 2014.

Dwork, C., McSherry, F., Nissim, K., and Smith, A. Calibrating noise to sensitivity in private data analysis. In *Theory of cryptography conference*, pp. 265–284. Springer, 2006.

Homer, N., Szelinger, S., Redman, M., Duggan, D., Tembe, W., Muehling, J., Pearson, J. V., Stephan, D. A., Nelson, S. F., and Craig, D. W. Resolving individuals contributing trace amounts of dna to highly complex mixtures using high-density snp genotyping microarrays. *PLoS genetics*, 4(8):e100167, 2008.

Jagielski, M., Ullman, J., and Oprea, A. Auditing differentially private machine learning: How private is private sgd? *Advances in Neural Information Processing Systems*, 33:22205–22216, 2020.

Jagielski, M., Wu, S., Oprea, A., Ullman, J., and Geambasu, R. How to Combine Membership-Inference Attacks on Multiple Updated Machine Learning Models. *Proceedings on Privacy Enhancing Technologies*, 2023(3):211–232, July 2023. ISSN 2299-0984. doi: 10.56553/popets-2023-0078.

Jayaraman, B. and Evans, D. Evaluating differentially private machine learning in practice. In *28th USENIX Security Symposium*, pp. 1895–1912, 2019.

Kairouz, P., Oh, S., and Viswanath, P. The composition theorem for differential privacy. In *International conference on machine learning*, pp. 1376–1385. PMLR, 2015.

Kiefer, J. and Wolfowitz, J. Stochastic estimation of the maximum of a regression function. *The Annals of Mathematical Statistics*, pp. 462–466, 1952.

Koskela, A. and Mohammadi, J. Auditing Differential Privacy Guarantees Using Density Estimation, October 2024.

Krizhevsky, A., Hinton, G., et al. Learning multiple layers of features from tiny images. 2009.

Leemann, T., Pawelczyk, M., and Kasneci, G. Gaussian membership inference privacy. *Advances in Neural Information Processing Systems*, 36:73866–73878, 2023.

Maddock, S., Sablayrolles, A., and Stock, P. CANIFE: Crafting Canaries for Empirical Privacy Measurement in Federated Learning, March 2023.

Massart, P. The tight constant in the dvoretzky-kiefer-wolfowitz inequality. *Annals of Probability*, 18, 1990.

Nasr, M., Songi, S., Thakurta, A., Papernot, N., and Carlini, N. Adversary instantiation: Lower bounds for differentially private machine learning. In *2021 IEEE Symposium on Security and Privacy (SP)*, pp. 866–882. IEEE, 2021.

Nasr, M., Hayes, J., Steinke, T., Balle, B., Tramèr, F., Jagielski, M., Carlini, N., and Terzis, A. Tight Auditing of Differentially Private Machine Learning, February 2023.

Neyman, J. and Pearson, E. S. IX. on the problem of the most efficient tests of statistical hypotheses. *Philosophical Transactions of the Royal Society of London. Series A, Containing Papers of a Mathematical or Physical Character*, 231(694–706):289–337, 1933.

Sablayrolles, A., Douze, M., Schmid, C., Ollivier, Y., and Jégou, H. White-box vs black-box: Bayes optimal strategies for membership inference. In *International Conference on Machine Learning*, pp. 5558–5567. PMLR, 2019.

Salem, A., Bhattacharya, A., Backes, M., Fritz, M., and Zhang, Y. Updates-leak: Data set inference and reconstruction attacks in online learning. In *29th USENIX Security Symposium*, pp. 1291–1308, 2020.

Sankararaman, S., Obozinski, G., Jordan, M. I., and Halperin, E. Genomic privacy and limits of individual detection in a pool. *Nature genetics*, 41(9):965–967, 2009.

Shokri, R., Stronati, M., Song, C., and Shmatikov, V. Membership inference attacks against machine learning models. In *2017 IEEE symposium on security and privacy (SP)*, pp. 3–18. IEEE, 2017.

Simonyan, K. and Zisserman, A. Very deep convolutional networks for large-scale image recognition. *arXiv preprint arXiv:1409.1556*, 2014.

Steinke, T., Nasr, M., and Jagielski, M. Privacy Auditing with One (1) Training Run, May 2023.

Tramer, F., Terzis, A., Steinke, T., Song, S., Jagielski, M., and Carlini, N. Debugging differential privacy: A case study for privacy auditing. *arXiv preprint arXiv:2202.12219*, 2022.

Van Trees, H. L. *Detection, estimation, and modulation theory, part I: detection, estimation, and linear modulation theory*. John Wiley & Sons, 2004.

Wasserman, L. and Zhou, S. A statistical framework for differential privacy. *Journal of the American Statistical Association*, 105(489):375–389, 2010.

Xiao, H., Rasul, K., and Vollgraf, R. Fashion-mnist: a novel image dataset for benchmarking machine learning algorithms. *arXiv preprint arXiv:1708.07747*, 2017.

Ye, J., Maddi, A., Murakonda, S. K., Bindschaedler, V., and Shokri, R. Enhanced membership inference attacks against machine learning models. In *Proceedings of the 2022 ACM SIGSAC conference on computer and communications security*, pp. 3093–3106, 2022.

Zanella-Béguelin, S., Wutschitz, L., Tople, S., Rühle, V., Paverd, A., Ohrimenko, O., Köpf, B., and Brockschmidt, M. Analyzing information leakage of updates to natural language models. In *Proceedings of the 2020 ACM SIGSAC conference on computer and communications security*, pp. 363–375, 2020.

Zeitouni, O., Ziv, J., and Merhav, N. When is the generalized likelihood ratio test optimal? *IEEE Transactions on Information Theory*, 38(5):1597–1602, 2002.

## A. Proofs for the Optimal Test

We consider  $T$  batches of size  $n$  drawn from  $\mathcal{D} = \mathcal{N}(\mu, \sigma^2)$  with known parameters  $(\mu, \sigma^2)$ . The target  $z^* \in \mathbb{R}$  is fixed. We test  $\mathbf{H}_0$  against  $\mathbf{H}_1^\tau$ , where  $\mathbf{H}_0$  is the null hypothesis that  $z^*$  is not in  $D_\tau$  and  $\mathbf{H}_1^\tau$  is the alternative hypothesis that  $z^*$  is in  $D_\tau$ . The insertion time  $\tau \in \{1, \dots, T\}$  is assumed known.

**Notation.** We write  $\bar{X}_t = \frac{1}{n} \sum_{k=1}^n X_{t,k}$  for the batch mean and  $\hat{\mu}_t = \frac{1}{tn} \sum_{j=1}^t \sum_{k=1}^n X_{j,k}$  for the cumulative empirical mean, which satisfies the recursion  $\hat{\mu}_t = \frac{t-1}{t} \hat{\mu}_{t-1} + \frac{1}{t} \bar{X}_t$ .

### A.1. Proof of Lemma 3.2

**Lemma 3.2.** *The likelihood ratio for testing  $\mathbf{H}_0$  against  $\mathbf{H}_1^\tau$  based on  $(\hat{\mu}_1, \dots, \hat{\mu}_T)$  satisfies*

$$\frac{p(\hat{\mu}_1, \dots, \hat{\mu}_T \mid \mathbf{H}_1^\tau)}{p(\hat{\mu}_1, \dots, \hat{\mu}_T \mid \mathbf{H}_0)} = \frac{p(\hat{\mu}_\tau \mid \hat{\mu}_{\tau-1}, \mathbf{H}_1^\tau)}{p(\hat{\mu}_\tau \mid \hat{\mu}_{\tau-1}, \mathbf{H}_0)}.$$

*Proof.* The likelihood ratio factorizes using the chain rule for conditional densities:

$$\text{LR}_\tau = \frac{p(\hat{\mu}_1, \dots, \hat{\mu}_T \mid \mathbf{H}_1^\tau)}{p(\hat{\mu}_1, \dots, \hat{\mu}_T \mid \mathbf{H}_0)} = \prod_{t=1}^T \frac{p(\hat{\mu}_t \mid \hat{\mu}_1, \dots, \hat{\mu}_{t-1}, \mathbf{H}_1^\tau)}{p(\hat{\mu}_t \mid \hat{\mu}_1, \dots, \hat{\mu}_{t-1}, \mathbf{H}_0)}.$$

The recursive relation  $\hat{\mu}_t = \frac{t-1}{t} \hat{\mu}_{t-1} + \frac{1}{t} \bar{X}_t$  implies that, given  $\hat{\mu}_{t-1}$ , the distribution of  $\hat{\mu}_t$  depends only on the distribution of the new batch mean  $\bar{X}_t$ . Earlier observations  $\hat{\mu}_1, \dots, \hat{\mu}_{t-2}$  provide no additional information once  $\hat{\mu}_{t-1}$  is known.

**Terms for  $t \neq \tau$  cancel.** For  $t < \tau$ , the target  $z^*$  has not yet been inserted into any batch. Under both  $\mathbf{H}_0$  and  $\mathbf{H}_1^\tau$ , all samples in batches  $D_1, \dots, D_t$  are drawn i.i.d. from  $\mathcal{D}$ . The conditional distribution of  $\hat{\mu}_t$  given  $\hat{\mu}_{t-1}$  is therefore identical under both hypotheses, and the corresponding factor in the product equals 1.

For  $t > \tau$ , the batch  $D_t$  contains no target sample under either hypothesis. Although the effect of  $z^*$  is present in  $\hat{\mu}_{t-1}$  under  $\mathbf{H}_1^\tau$ , conditioning on  $\hat{\mu}_{t-1}$  absorbs this effect. The new batch  $\bar{X}_t$  is drawn from  $\mathcal{N}(\mu, \sigma^2/n)$  under both hypotheses, so the conditional distributions of  $\hat{\mu}_t$  given  $\hat{\mu}_{t-1}$  are again identical. These factors also equal 1.

The only factor that differs between the two hypotheses is the one at  $t = \tau$ , where the batch  $D_\tau$  contains  $z^*$  under  $\mathbf{H}_1^\tau$  but not under  $\mathbf{H}_0$ .  $\square$

### A.2. Proof of Theorem 3.4

**Theorem 3.4 (Log Likelihood Ratio).** *The log likelihood ratio for univariate samples has the form*

$$\begin{aligned} \log \text{LR}_\tau &= -\frac{1}{2} \log \left( \frac{n-1}{n} \right) - \frac{n}{2(n-1)\sigma^2} (\bar{X}_\tau - \mu)^2 \\ &\quad + \frac{(z^* - \mu)n}{(n-1)\sigma^2} (\bar{X}_\tau - \mu) - \frac{(z^* - \mu)^2}{2(n-1)\sigma^2}. \end{aligned}$$

*Proof.* We derive the log likelihood ratio from the conditional distributions at time  $\tau$ .

**Conditional distributions.** From the main text, the conditional distributions are:

$$\begin{aligned} \hat{\mu}_\tau \mid \hat{\mu}_{\tau-1}, \mathbf{H}_0 &\sim \mathcal{N}(m_0, v_0) \\ \hat{\mu}_\tau \mid \hat{\mu}_{\tau-1}, \mathbf{H}_1^\tau &\sim \mathcal{N}(m_1, v_1) \end{aligned}$$

where

$$\begin{aligned} m_0 &= \frac{\tau-1}{\tau} \hat{\mu}_{\tau-1} + \frac{\mu}{\tau}, & v_0 &= \frac{\sigma^2}{\tau^2 n}, \\ m_1 &= \frac{\tau-1}{\tau} \hat{\mu}_{\tau-1} + \frac{(n-1)\mu + z^*}{\tau n}, & v_1 &= \frac{(n-1)\sigma^2}{\tau^2 n^2}. \end{aligned}$$

**Log likelihood ratio.** Let  $N = \hat{\mu}_\tau - m_0$ . The log likelihood ratio between two Gaussians is:

$$\log \text{LR}_\tau = -\frac{1}{2} \log \left( \frac{v_1}{v_0} \right) + \frac{N^2}{2v_0} - \frac{(N - (m_1 - m_0))^2}{2v_1}.$$

Expanding  $(N - (m_1 - m_0))^2$ :

$$\log \text{LR}_\tau = -\frac{1}{2} \log \left( \frac{v_1}{v_0} \right) + N^2 \left( \frac{1}{2v_0} - \frac{1}{2v_1} \right) + \frac{N(m_1 - m_0)}{v_1} - \frac{(m_1 - m_0)^2}{2v_1}.$$

**Variance ratio and mean difference.** The variance ratio is:

$$\frac{v_1}{v_0} = \frac{(n-1)\sigma^2/(\tau^2 n^2)}{\sigma^2/(\tau^2 n)} = \frac{n-1}{n}.$$

The mean difference is:

$$m_1 - m_0 = \frac{(n-1)\mu + z^*}{\tau n} - \frac{\mu}{\tau} = \frac{(n-1)\mu + z^* - n\mu}{\tau n} = \frac{z^* - \mu}{\tau n}.$$

**Simplification.** Using  $N = \frac{1}{\tau}(\bar{X}_\tau - \mu)$  and computing the coefficients:

$$\begin{aligned} \frac{1}{2v_0} - \frac{1}{2v_1} &= \frac{\tau^2 n}{2\sigma^2} - \frac{\tau^2 n^2}{2(n-1)\sigma^2} = -\frac{\tau^2 n}{2(n-1)\sigma^2}, \\ \frac{m_1 - m_0}{v_1} &= \frac{(z^* - \mu)\tau n}{(n-1)\sigma^2}, \\ \frac{(m_1 - m_0)^2}{2v_1} &= \frac{(z^* - \mu)^2}{2(n-1)\sigma^2}. \end{aligned}$$

Substituting  $N\tau = \bar{X}_\tau - \mu$ , the  $\tau$  factors cancel in the quadratic and linear terms, yielding:

$$\log \text{LR}_\tau = -\frac{1}{2} \log \left( \frac{n-1}{n} \right) - \frac{n}{2(n-1)\sigma^2}(\bar{X}_\tau - \mu)^2 + \frac{(z^* - \mu)n}{(n-1)\sigma^2}(\bar{X}_\tau - \mu) - \frac{(z^* - \mu)^2}{2(n-1)\sigma^2}.$$

□

### A.3. Proof of Lemma 3.5

**Lemma 3.5** (Type I Error). Define  $\gamma_{\max} = \frac{1}{2} \left[ \frac{(z^* - \mu)^2}{\sigma^2} - \log \left( \frac{n-1}{n} \right) \right]$ . For  $\gamma > \gamma_{\max}$ , we have  $\alpha(\gamma) = 0$ . For  $\gamma \leq \gamma_{\max}$ :

$$\alpha(\gamma) = \Phi(a + b(\gamma)) - \Phi(a - b(\gamma))$$

where  $m^* = \frac{(z^* - \mu)^2}{\sigma^2}$ ,  $a = \sqrt{m^* n}$  and  $b(\gamma) = \sqrt{(n-1)(m^* - \log(1 - \frac{1}{n}) - 2\gamma)}$ .

*Proof.* The test statistic has the quadratic form  $\log \text{LR}_\tau = c_0 + c_1 N + c_2 N^2$  where  $c_2 < 0$ .

The condition  $\log \text{LR}_\tau \geq \gamma$  is equivalent to  $c_2 N^2 + c_1 N + (c_0 - \gamma) \geq 0$ . Since  $c_2 < 0$ , this downward-opening parabola is non-negative only when  $N$  lies between its two roots (if they exist).

The discriminant of the quadratic is:

$$\Delta = c_1^2 - 4c_2(c_0 - \gamma) = \frac{\tau^2 n}{\sigma^2(n-1)} \left[ \frac{(z^* - \mu)^2}{\sigma^2} - \log \left( \frac{n-1}{n} \right) - 2\gamma \right].$$

**Case 1:** If  $\Delta < 0$ , the parabola never reaches zero, so  $\alpha = 0$ . This occurs when  $\gamma > \gamma_{\max}$ .

**Case 2:** For  $\Delta \geq 0$ , the roots are:

$$N_{1,2} = \frac{z^* - \mu}{\tau} \mp \frac{\sigma\sqrt{n-1}}{\tau\sqrt{n}} \sqrt{\frac{(z^* - \mu)^2}{\sigma^2} - \log\left(\frac{n-1}{n}\right) - 2\gamma}.$$

Under  $\mathbf{H}_0$ ,  $N \sim \mathcal{N}(0, \sigma^2/(\tau^2 n))$ . The Type I error is:

$$\alpha(\gamma) = P_0(N_1 \leq N \leq N_2) = \Phi\left(\frac{N_2}{\sigma/(\tau\sqrt{n})}\right) - \Phi\left(\frac{N_1}{\sigma/(\tau\sqrt{n})}\right).$$

Substituting the expressions for  $N_1$  and  $N_2$  and simplifying (noting that  $\tau$  cancels) yields the stated formula with  $a = \frac{(z^* - \mu)\sqrt{n}}{\sigma}$  and  $b(\gamma) = \sqrt{n-1} \sqrt{\frac{(z^* - \mu)^2}{\sigma^2} - \log\left(\frac{n-1}{n}\right) - 2\gamma}$ .  $\square$

#### A.4. Proof of Lemma 3.6

**Lemma 3.6** (Type II Error). *For  $\gamma \leq \gamma_{\max}$ , with  $a$  and  $b(\gamma)$  as defined above:*

$$\begin{aligned} \beta(\gamma) &= \Phi\left(a\sqrt{\frac{n-1}{n}} - b(\gamma)\sqrt{\frac{n}{n-1}}\right) \\ &\quad + \Phi\left(-a\sqrt{\frac{n-1}{n}} - b(\gamma)\sqrt{\frac{n}{n-1}}\right) \end{aligned}$$

*Proof.* The Type II error is  $\beta(\gamma) = P_1(\log \text{LR}_\tau < \gamma) = P_1(N < N_1) + P_1(N > N_2)$ .

Under  $\mathbf{H}_1^T$ , the batch mean is  $\bar{X}_\tau \sim \mathcal{N}\left(\frac{(n-1)\mu + z^*}{n}, \frac{(n-1)\sigma^2}{n^2}\right)$ . Therefore:

$$N = \frac{1}{\tau}(\bar{X}_\tau - \mu) \sim \mathcal{N}\left(\frac{z^* - \mu}{\tau n}, \frac{(n-1)\sigma^2}{\tau^2 n^2}\right).$$

Let  $\mu_1 = \frac{z^* - \mu}{\tau n}$  and  $\sigma_1 = \frac{\sigma\sqrt{n-1}}{\tau n}$ . Then:

$$\beta(\gamma) = \Phi\left(\frac{N_1 - \mu_1}{\sigma_1}\right) + \Phi\left(\frac{-(N_2 - \mu_1)}{\sigma_1}\right).$$

From the expressions for  $N_{1,2}$  and after algebraic simplification:

$$\frac{N_{1,2} - \mu_1}{\sigma_1} = \frac{(z^* - \mu)\sqrt{n-1}}{\sigma} \mp \sqrt{n} \sqrt{\frac{(z^* - \mu)^2}{\sigma^2} - \log\left(\frac{n-1}{n}\right) - 2\gamma}.$$

This yields the stated formula.  $\square$

#### A.5. Proof of Lemma 3.7

**Lemma 3.7** (Final Observation Type I Error). *For the Final Observation test with  $\gamma_{\max}^{(T)} = \frac{1}{2} \left[ \frac{(z^* - \mu)^2}{\sigma^2} - \log\left(\frac{nT-1}{nT}\right) \right]$  and  $\gamma \leq \gamma_{\max}^{(T)}$ , the Type I error*

$$\alpha_{\text{FO}}(\gamma) = \Phi(a_T + b_T(\gamma)) - \Phi(a_T - b_T(\gamma))$$

where  $a_T = \sqrt{m^* n T}$  and  $b_T(\gamma) = \sqrt{(nT-1)(m^* - \log(1 - \frac{1}{nT}) - 2\gamma)}$ .

*Proof.* The proof follows the same structure as Lemma 3.5, with  $n$  replaced by  $nT$  throughout.

For the single-observation case, the test statistic is  $\log \text{LR} = c_0^{(T)} + c_1^{(T)}W + c_2^{(T)}W^2$  where  $W = \hat{\mu}_T - \mu$  and:

$$\begin{aligned} c_0^{(T)} &= -\frac{1}{2} \log \left( \frac{nT-1}{nT} \right) - \frac{(z^* - \mu)^2}{2(nT-1)\sigma^2}, \\ c_1^{(T)} &= \frac{nT(z^* - \mu)}{(nT-1)\sigma^2}, \\ c_2^{(T)} &= -\frac{nT}{2(nT-1)\sigma^2}. \end{aligned}$$

The discriminant is:

$$\Delta = \frac{nT}{\sigma^2(nT-1)} \left[ \frac{(z^* - \mu)^2}{\sigma^2} - \log \left( \frac{nT-1}{nT} \right) - 2\gamma \right].$$

For  $\Delta \geq 0$ , the roots are:

$$W_{1,2} = \frac{z^* - \mu}{nT} \mp \frac{\sigma\sqrt{nT-1}}{nT} \sqrt{\frac{(z^* - \mu)^2}{\sigma^2} - \log \left( \frac{nT-1}{nT} \right) - 2\gamma}.$$

Under  $\mathbf{H}_0$ ,  $W \sim \mathcal{N}(0, \sigma^2/(nT))$ , giving the stated formula.  $\square$

#### A.6. Proof of Lemma 3.8

**Lemma 3.8** (Final Observation Type II Error). *For  $\gamma \leq \gamma_{\max}^{(T)}$ , with  $a_T$  and  $b_T(\gamma)$  as defined above, the Type II error*

$$\begin{aligned} \beta_{\text{FO}}(\gamma) &= \Phi \left( a_T \sqrt{\frac{nT-1}{nT}} - b_T(\gamma) \sqrt{\frac{nT}{nT-1}} \right) \\ &+ \Phi \left( -a_T \sqrt{\frac{nT-1}{nT}} - b_T(\gamma) \sqrt{\frac{nT}{nT-1}} \right). \end{aligned}$$

*Proof.* Under  $\mathbf{H}_1^\tau$ , one sample among  $nT$  is replaced by  $z^*$ :

$$W = \hat{\mu}_T - \mu \sim \mathcal{N} \left( \frac{z^* - \mu}{nT}, \frac{(nT-1)\sigma^2}{(nT)^2} \right).$$

The Type II error  $\beta(\gamma) = P_1(W < W_1) + P_1(W > W_2)$  follows by the same calculation as Lemma 3.6, with  $n$  replaced by  $nT$ .  $\square$

## B. Multivariate Gaussian Extension

We extend the sequential membership inference approach to the multivariate Gaussian setting where datapoints lie in  $\mathbb{R}^d$ . We consider  $T$  batches of size  $n$  drawn from  $\mathcal{D} = \mathcal{N}(\boldsymbol{\mu}, \boldsymbol{\Sigma})$  where  $\boldsymbol{\mu} \in \mathbb{R}^d$  and  $\boldsymbol{\Sigma} \in \mathbb{R}^{d \times d}$  is positive definite and known. The target  $\mathbf{z}^* \in \mathbb{R}^d$  and  $\tau$  are known. We test  $\mathbf{H}_0$  versus  $\mathbf{H}_1^\tau$  as defined in (4).

**Notation.** Bold symbols denote vectors ( $\mathbf{x} \in \mathbb{R}^d$ ) and matrices ( $\boldsymbol{\Sigma} \in \mathbb{R}^{d \times d}$ ). The Mahalanobis distance is  $\|\mathbf{x}\|_{\boldsymbol{\Sigma}} = \sqrt{\mathbf{x}^\top \boldsymbol{\Sigma}^{-1} \mathbf{x}}$ .

### B.1. Conditional Distributions

The recursive relation  $\hat{\boldsymbol{\mu}}_t = \frac{t-1}{t}\hat{\boldsymbol{\mu}}_{t-1} + \frac{1}{t}\bar{\mathbf{X}}_t$  extends naturally.

**Lemma B.1** (Multivariate Conditional Distributions). *The conditional distributions at time  $\tau$  are:*

$$\begin{aligned} \hat{\boldsymbol{\mu}}_\tau \mid \hat{\boldsymbol{\mu}}_{\tau-1}, \mathbf{H}_0 &\sim \mathcal{N} \left( \frac{\tau-1}{\tau} \hat{\boldsymbol{\mu}}_{\tau-1} + \frac{\boldsymbol{\mu}}{\tau}, \frac{\boldsymbol{\Sigma}}{\tau^2 n} \right), \\ \hat{\boldsymbol{\mu}}_\tau \mid \hat{\boldsymbol{\mu}}_{\tau-1}, \mathbf{H}_1^\tau &\sim \mathcal{N} \left( \frac{\tau-1}{\tau} \hat{\boldsymbol{\mu}}_{\tau-1} + \frac{(n-1)\boldsymbol{\mu} + \mathbf{z}^*}{\tau n}, \frac{(n-1)\boldsymbol{\Sigma}}{\tau^2 n^2} \right). \end{aligned}$$

*Proof.* **Batch mean distributions.** Under  $\mathbf{H}_0$ , the batch mean is  $\bar{\mathbf{X}}_\tau \sim \mathcal{N}(\boldsymbol{\mu}, \boldsymbol{\Sigma}/n)$ .

Under  $\mathbf{H}_1^\tau$ , the batch contains  $(n-1)$  samples from  $\mathcal{D}$  plus  $\mathbf{z}^*$ :

$$\bar{\mathbf{X}}_\tau = \frac{1}{n} [(n-1)\boldsymbol{\mu}_{\text{sample}} + \mathbf{z}^*]$$

where  $\boldsymbol{\mu}_{\text{sample}} \sim \mathcal{N}(\boldsymbol{\mu}, \boldsymbol{\Sigma}/(n-1))$ . The result follows.

The recursion  $\hat{\boldsymbol{\mu}}_\tau = \frac{\tau-1}{\tau} \hat{\boldsymbol{\mu}}_{\tau-1} + \frac{1}{\tau} \bar{\mathbf{X}}_\tau$  is an affine transformation, yielding the stated conditional distributions.  $\square$

## B.2. Log Likelihood Ratio

**Theorem B.2** (Multivariate Log Likelihood Ratio). *Define  $\mathbf{N}_\tau = \tau(\hat{\boldsymbol{\mu}}_\tau - \frac{\tau-1}{\tau} \hat{\boldsymbol{\mu}}_{\tau-1} - \frac{\boldsymbol{\mu}}{\tau}) = \bar{\mathbf{X}}_\tau - \boldsymbol{\mu}$ . The log likelihood ratio is:*

$$\begin{aligned} \log \text{LR}_\tau &= -\frac{d}{2} \log \left( \frac{n-1}{n} \right) - \frac{n}{2(n-1)} \mathbf{N}_\tau^\top \boldsymbol{\Sigma}^{-1} \mathbf{N}_\tau \\ &\quad + \frac{n}{n-1} \mathbf{N}_\tau^\top \boldsymbol{\Sigma}^{-1} (\mathbf{z}^* - \boldsymbol{\mu}) - \frac{(\mathbf{z}^* - \boldsymbol{\mu})^\top \boldsymbol{\Sigma}^{-1} (\mathbf{z}^* - \boldsymbol{\mu})}{2(n-1)}. \end{aligned}$$

*Proof.* **Conditional parameters.** Let  $\mathbf{m}_0, \mathbf{m}_1$  be the conditional means and  $\mathbf{V}_0 = \frac{\boldsymbol{\Sigma}}{\tau^2 n}$ ,  $\mathbf{V}_1 = \frac{(n-1)\boldsymbol{\Sigma}}{\tau^2 n^2}$  the conditional covariances.

**Covariance ratio and mean difference.** We have  $\mathbf{V}_1 = \frac{n-1}{n} \mathbf{V}_0$ , so  $\det(\mathbf{V}_1) = \left(\frac{n-1}{n}\right)^d \det(\mathbf{V}_0)$  and  $\mathbf{V}_1^{-1} = \frac{n}{n-1} \mathbf{V}_0^{-1}$ . The mean difference is:

$$\mathbf{m}_1 - \mathbf{m}_0 = \frac{(n-1)\boldsymbol{\mu} + \mathbf{z}^*}{\tau n} - \frac{\boldsymbol{\mu}}{\tau} = \frac{\mathbf{z}^* - \boldsymbol{\mu}}{\tau n}.$$

**Log likelihood ratio.** The multivariate Gaussian log likelihood ratio is:

$$\log \text{LR}_\tau = -\frac{1}{2} \log \frac{\det(\mathbf{V}_1)}{\det(\mathbf{V}_0)} + \frac{1}{2} \mathbf{L}_\tau^\top \mathbf{V}_0^{-1} \mathbf{L}_\tau - \frac{1}{2} (\mathbf{L}_\tau - (\mathbf{m}_1 - \mathbf{m}_0))^\top \mathbf{V}_1^{-1} (\mathbf{L}_\tau - (\mathbf{m}_1 - \mathbf{m}_0))$$

where  $\mathbf{L}_\tau = \hat{\boldsymbol{\mu}}_\tau - \mathbf{m}_0 = \frac{1}{\tau} \mathbf{N}_\tau$ . The determinant term gives  $-\frac{d}{2} \log \left( \frac{n-1}{n} \right)$ . Expanding the quadratic terms with  $\mathbf{V}_0^{-1} = \tau^2 n \boldsymbol{\Sigma}^{-1}$  and simplifying yields the stated result.  $\square$

**Corollary B.3** (Quadratic Form). *The log likelihood ratio has the form  $\log \text{LR}_\tau = c_0 + \mathbf{c}_1^\top \mathbf{N}_\tau + \mathbf{N}_\tau^\top \mathbf{C}_2 \mathbf{N}_\tau$  where:*

$$\begin{aligned} c_0 &= -\frac{d}{2} \log \left( \frac{n-1}{n} \right) - \frac{m^*}{2(n-1)}, \\ \mathbf{c}_1 &= \frac{n}{n-1} \boldsymbol{\Sigma}^{-1} (\mathbf{z}^* - \boldsymbol{\mu}), \\ \mathbf{C}_2 &= -\frac{n}{2(n-1)} \boldsymbol{\Sigma}^{-1}, \end{aligned}$$

and  $m^* = (\mathbf{z}^* - \boldsymbol{\mu})^\top \boldsymbol{\Sigma}^{-1} (\mathbf{z}^* - \boldsymbol{\mu})$  is the squared Mahalanobis distance.

## B.3. Type I and II Error Analysis

**Lemma B.4** (Distributions of the Test Statistic). *Under  $\mathbf{H}_0$ :  $\mathbf{N}_\tau \sim \mathcal{N}(\mathbf{0}, \frac{\boldsymbol{\Sigma}}{n})$ .*

*Under  $\mathbf{H}_1^\tau$ :  $\mathbf{N}_\tau \sim \mathcal{N}\left(\frac{\mathbf{z}^* - \boldsymbol{\mu}}{n}, \frac{(n-1)\boldsymbol{\Sigma}}{n^2}\right)$ .*

**Lemma B.5** (Type I Error Analysis - Diagonal Case). *For the log likelihood ratio test with threshold  $\gamma$  in the multivariate Gaussian case with diagonal covariance  $\boldsymbol{\Sigma} = \text{diag}(\sigma_1^2, \dots, \sigma_d^2)$ , let:*

$$\gamma_{\max} = \frac{1}{2} \left[ m^* - d \log \left( \frac{n-1}{n} \right) \right]$$

where  $m^* = \sum_{j=1}^d \frac{(z_j^* - \mu_j)^2}{\sigma_j^2}$  is the squared Mahalanobis distance. For  $\gamma \leq \gamma_{\max}$ , the Type I error is:

$$\alpha(\gamma) = \mathbb{P}_0 (\|\mathbf{U}\|_{\Sigma^{-1}}^2 \leq R^2(\gamma))$$

where  $\mathbf{U} \sim \mathcal{N}(-(\mathbf{z}^* - \boldsymbol{\mu}), \frac{\Sigma}{n})$  and  $R^2(\gamma) = \frac{2(n-1)}{n} \left[ \frac{n^2 m^*}{2} - \gamma - \frac{d}{2} \log \left( \frac{n-1}{n} \right) \right]$ .

*Proof.* With diagonal covariance, the log likelihood ratio sums over dimensions:  $\log \text{LR}_\tau = \sum_{j=1}^d \log \text{LR}_{\tau,j}$ . The sum can be written as  $\log \text{LR}_\tau = \mathbf{N}_\tau^\top \mathbf{C}_2 \mathbf{N}_\tau + \mathbf{c}_1^\top \mathbf{N}_\tau + c_0$  with diagonal  $\mathbf{C}_2$ .

Substituting the coefficients from Corollary B.3 (adapted for diagonal  $\Sigma$ ), we complete the square. Let  $\mathbf{M}_\tau = \mathbf{N}_\tau - (\mathbf{z}^* - \boldsymbol{\mu})$ . Under  $\mathbf{H}_0$ ,  $\mathbf{N}_\tau \sim \mathcal{N}(\mathbf{0}, \Sigma/n)$ , so  $\mathbf{M}_\tau \sim \mathcal{N}(-(\mathbf{z}^* - \boldsymbol{\mu}), \Sigma/n)$ .

The condition  $\log \text{LR}_\tau \geq \gamma$  transforms to:

$$\mathbf{M}_\tau^\top \mathbf{C}_2 \mathbf{M}_\tau \geq \gamma - c_0 + \frac{1}{4} \mathbf{c}_1^\top \mathbf{C}_2^{-1} \mathbf{c}_1.$$

Substituting the specific values for  $c_0, \mathbf{c}_1, \mathbf{C}_2$ , the RHS simplifies to  $\gamma + \frac{d}{2} \log \left( \frac{n-1}{n} \right) - \frac{n^2 m^*}{2}$ .

Since  $\mathbf{C}_2 = -\frac{n}{2(n-1)} \Sigma^{-1}$  is negative definite, the inequality reverses:

$$\mathbf{M}_\tau^\top \Sigma^{-1} \mathbf{M}_\tau \leq -\frac{2(n-1)}{n} \left[ \gamma + \frac{d}{2} \log \left( \frac{n-1}{n} \right) - \frac{n^2 m^*}{2} \right].$$

Letting  $\mathbf{U} = \mathbf{M}_\tau$ , the result follows. The probability is the mass of a shifted Gaussian within an ellipsoid defined by the Mahalanobis distance.  $\square$

**Corollary B.6** (Explicit Type I Error). *For diagonal covariance  $\Sigma = \text{diag}(\sigma_1^2, \dots, \sigma_d^2)$ , the Type I error is:*

$$\alpha(\gamma) = F_{\chi_d^2(\lambda)}(n R^2(\gamma))$$

where  $F_{\chi_d^2(\lambda)}$  is the CDF of the non-central chi-squared distribution with  $d$  degrees of freedom and non-centrality parameter  $\lambda = nm^*$ , and  $R^2(\gamma)$  is defined as in Lemma 3.5.

*Proof.* For diagonal  $\Sigma$ , the squared Mahalanobis norm decomposes as  $\|\mathbf{U}\|_{\Sigma^{-1}}^2 = \sum_{j=1}^d U_j^2 / \sigma_j^2$ . Each component  $U_j \sim \mathcal{N}(-z_j^* + \mu_j, \sigma_j^2/n)$ , so the standardized variable  $W_j = \sqrt{n} U_j / \sigma_j \sim \mathcal{N}(-\sqrt{n}(z_j^* - \mu_j) / \sigma_j, 1)$ .

The sum  $\sum_{j=1}^d W_j^2 = n \|\mathbf{U}\|_{\Sigma^{-1}}^2$  follows a non-central chi-squared distribution with  $d$  degrees of freedom and non-centrality parameter  $\lambda = \sum_{j=1}^d n(z_j^* - \mu_j)^2 / \sigma_j^2 = nm^*$ .  $\square$

## C. Robustness to Distribution Shift

We consider the setting where each batch may be drawn from a different distribution:  $D_t \sim \mathcal{N}(\mu_t, \sigma_t^2)$  for  $t = 1, \dots, T$ . The target  $z^* \in \mathbb{R}$  and the insertion time  $\tau$  are fixed. We test  $\mathbf{H}_0$  versus  $\mathbf{H}_1^\tau$ .

**Notation.** Parameters  $(\mu_t, \sigma_t^2)$  may vary with  $t$ , but only  $(\mu_\tau, \sigma_\tau^2)$  at the insertion time affect the test.

### C.1. Main Result

**Theorem C.1** (Robustness to Distribution Shift). *The likelihood ratio test for  $\mathbf{H}_0 : z^* \notin D_\tau$  versus  $\mathbf{H}_1^\tau : z^* \in D_\tau$  depends only on  $(\mu_\tau, \sigma_\tau^2)$ . The distributions of batches  $D_t$  for  $t \neq \tau$  do not affect the test.*

*Proof. Likelihood ratio decomposition.* The cumulative empirical mean satisfies  $\hat{\mu}_t = \frac{t-1}{t} \hat{\mu}_{t-1} + \frac{1}{t} \bar{X}_t$ . The likelihood ratio decomposes as:

$$\text{LR} = \prod_{t=1}^T \frac{p(\hat{\mu}_t \mid \hat{\mu}_{t-1}, \mathbf{H}_1^\tau)}{p(\hat{\mu}_t \mid \hat{\mu}_{t-1}, \mathbf{H}_0)}.$$

**Terms for  $t \neq \tau$  cancel.** For  $t < \tau$ , the target has not been inserted. Under both hypotheses, batch  $D_t$  is drawn from  $\mathcal{N}(\mu_t, \sigma_t^2)$ . The conditional distributions of  $\hat{\mu}_t$  given  $\hat{\mu}_{t-1}$  are identical under both hypotheses, so the corresponding factor equals 1.

For  $t > \tau$ , batch  $D_t$  contains no target under either hypothesis. Although the effect of  $z^*$  is present in  $\hat{\mu}_{t-1}$  under  $\mathbf{H}_1^\tau$ , conditioning on  $\hat{\mu}_{t-1}$  absorbs this effect. The batch  $\bar{X}_t$  is drawn from  $\mathcal{N}(\mu_t, \sigma_t^2/n)$  under both hypotheses, so the conditional distributions of  $\hat{\mu}_t$  given  $\hat{\mu}_{t-1}$  are identical. These factors also equal 1.

**The transition at  $t = \tau$ .** The only factor that differs is at  $t = \tau$ , where the conditional distributions are:

$$\begin{aligned}\hat{\mu}_\tau \mid \hat{\mu}_{\tau-1}, \mathbf{H}_0 &\sim \mathcal{N}\left(\frac{\tau-1}{\tau}\hat{\mu}_{\tau-1} + \frac{\mu_\tau}{\tau}, \frac{\sigma_\tau^2}{\tau^2 n}\right), \\ \hat{\mu}_\tau \mid \hat{\mu}_{\tau-1}, \mathbf{H}_1^\tau &\sim \mathcal{N}\left(\frac{\tau-1}{\tau}\hat{\mu}_{\tau-1} + \frac{(n-1)\mu_\tau + z^*}{\tau n}, \frac{(n-1)\sigma_\tau^2}{\tau^2 n^2}\right).\end{aligned}$$

These expressions involve only  $(\mu_\tau, \sigma_\tau^2)$ . The parameters  $(\mu_t, \sigma_t^2)$  for  $t \neq \tau$  do not appear in the likelihood ratio.  $\square$

## D. Proofs for Uniform $\tau$ Test

We derive the optimal test for  $\mathbf{H}_0$  against  $\widetilde{\mathbf{H}_1}$  where  $\tau \sim \text{Uniform}(\{1, \dots, T\})$ . As before,  $T$  batches of size  $n$  are drawn from  $\mathcal{D} = \mathcal{N}(\mu, \sigma^2)$  with known parameters.

**Notation.** We write  $\text{LR}_t$  for the likelihood ratio at time  $t$  (derived in Theorem 3.4) and  $\log \text{LR}_t$  for its logarithm. The batch means  $\bar{X}_1, \dots, \bar{X}_T$  are independent under both hypotheses.

### D.1. Derivation of the Likelihood Ratio

**Theorem 3.10** (Uniform  $\tau$  Likelihood Ratio). *Let  $\text{LR}_t$  be the likelihood ratio for  $\mathbf{H}_0$  against  $\mathbf{H}_1^t$  from Theorem 3.1. The likelihood ratio for testing  $\mathbf{H}_0$  against  $\widetilde{\mathbf{H}_1}$  is*

$$\text{LR}_{\text{Unif}} = \frac{1}{T} \sum_{t=1}^T \text{LR}_t.$$

*Proof.* Under  $\widetilde{\mathbf{H}_1}$ , the insertion time satisfies  $\mathbb{P}(\tau = t \mid \widetilde{\mathbf{H}_1}) = 1/T$ . The marginal likelihood of the observations is:

$$p(\hat{\mu}_1, \dots, \hat{\mu}_T \mid \widetilde{\mathbf{H}_1}) = \sum_{t=1}^T \mathbb{P}(\tau = t) \cdot p(\hat{\mu}_1, \dots, \hat{\mu}_T \mid \tau = t, \widetilde{\mathbf{H}_1}).$$

Conditioned on  $\tau = t$ , the data distribution matches  $\mathbf{H}_1^t$ :

$$p(\hat{\mu}_1, \dots, \hat{\mu}_T \mid \tau = t, \widetilde{\mathbf{H}_1}) = p(\hat{\mu}_1, \dots, \hat{\mu}_T \mid \mathbf{H}_1^t).$$

Dividing by the null likelihood:

$$\text{LR}_{\text{Unif}} = \frac{p(\hat{\mu}_1, \dots, \hat{\mu}_T \mid \widetilde{\mathbf{H}_1})}{p(\hat{\mu}_1, \dots, \hat{\mu}_T \mid \mathbf{H}_0)} = \frac{1}{T} \sum_{t=1}^T \frac{p(\hat{\mu}_1, \dots, \hat{\mu}_T \mid \mathbf{H}_1^t)}{p(\hat{\mu}_1, \dots, \hat{\mu}_T \mid \mathbf{H}_0)} = \frac{1}{T} \sum_{t=1}^T \text{LR}_t.$$

$\square$

Each  $\text{LR}_t$  depends on the data only through  $\bar{X}_t$  (by the isolation property), and batch means are independent. The test statistic aggregates evidence across all time steps.

## D.2. Log-Sum-Exp Form

**Corollary D.1** (Log Likelihood Ratio). *The log likelihood ratio is*

$$\log \text{LR}_{\text{Unif}} = \text{logsumexp}(\log \text{LR}_1, \dots, \log \text{LR}_T) - \log T$$

where  $\text{logsumexp}(x_1, \dots, x_T) = \log \left( \sum_{t=1}^T e^{x_t} \right)$ .

*Proof.* Taking the logarithm of Theorem 3.10:

$$\log \text{LR}_{\text{Unif}} = \log \left( \frac{1}{T} \sum_{t=1}^T \text{LR}_t \right) = \log \left( \sum_{t=1}^T e^{\log \text{LR}_t} \right) - \log T.$$

□

The log-sum-exp function is numerically stable:  $\text{logsumexp}(x_1, \dots, x_T) = m + \log \left( \sum_{t=1}^T e^{x_t - m} \right)$  where  $m = \max_t x_t$ .

## D.3. Relationship to the GLR Test

**Proposition D.2** (Bounds). *The log likelihood ratio satisfies*

$$\max_t \log \text{LR}_t - \log T \leq \log \text{LR}_{\text{Unif}} \leq \max_t \log \text{LR}_t.$$

*Proof.* **Upper bound.** Since  $\text{LR}_t \geq 0$ :

$$\frac{1}{T} \sum_{t=1}^T \text{LR}_t \leq \max_t \text{LR}_t.$$

**Lower bound.** The average is at least the maximum divided by  $T$ :

$$\frac{1}{T} \sum_{t=1}^T \text{LR}_t \geq \frac{1}{T} \max_t \text{LR}_t.$$

□

When one  $\text{LR}_{t^*}$  dominates,  $\log \text{LR}_{\text{Unif}} \approx \log \text{LR}_{t^*} - \log T$ . When multiple batches contribute comparable evidence, the test accumulates their contributions.

## E. Proofs for GLR test

Consider the case where  $T$  batches of size  $n$  are drawn from  $\mathcal{D} = \mathcal{N}(\mu, \sigma^2)$  with known parameters  $(\mu, \sigma^2)$ , but the insertion time is unknown. The target  $z^* \in \mathbb{R}$  is fixed. We test:

$\mathbf{H}_0$  : All datapoints sampled i.i.d. from  $\mathcal{D}$

$\widetilde{\mathbf{H}}_1$  : One sample in  $D_\tau$  replaced by  $z^*$  for some unknown  $\tau \in \{1, \dots, T\}$

**Notation.** We write  $\bar{X}_t$  for the batch mean,  $\hat{\mu}_t$  for the cumulative empirical mean, and  $\log \text{LR}_\tau$  for the log likelihood ratio at time  $\tau$ . The test statistic for  $\text{SeMI}^{\text{max}}$  is  $\max_\tau \log \text{LR}_\tau$ . Single-batch error rates are  $\alpha_0(\gamma) = P_0(\log \text{LR}_1 \geq \gamma)$  and  $\beta_0(\gamma) = P_1(\log \text{LR}_1 < \gamma)$ .

### E.1. Independence of Log Likelihood Ratios under $\mathbf{H}_0$

**Theorem E.1** (Independence under  $\mathbf{H}_0$ ). *Under  $\mathbf{H}_0$ , the statistics  $\log \text{LR}_1, \dots, \log \text{LR}_T$  are independent and identically distributed.*

*Proof.* From Theorem 3.4, each  $\log \text{LR}_\tau$  depends on the data only through  $\bar{X}_\tau - \mu$ . The coefficients  $c_0, c_1$ , and  $c_2$  in the quadratic form depend on  $n, \sigma^2, \mu$ , and  $z^*$ , but not on  $\tau$ .

Under  $\mathbf{H}_0$ , each batch  $D_\tau$  is sampled independently from  $\mathcal{N}(\mu, \sigma^2)^n$ . The batch means  $\bar{X}_1, \dots, \bar{X}_T$  are therefore independent random variables. Moreover, each  $\bar{X}_\tau \sim \mathcal{N}(\mu, \sigma^2/n)$  for all  $\tau \in \{1, \dots, T\}$ . Since the log likelihood ratio is a function of  $\bar{X}_\tau - \mu$  with coefficients that do not depend on  $\tau$ , the statistics  $\log \text{LR}_1, \dots, \log \text{LR}_T$  have the same distribution.

The statistics  $\log \text{LR}_\tau$  are functions of independent, identically distributed random variables (the batch means), and these functions are identical across  $\tau$ . Therefore,  $\log \text{LR}_1, \dots, \log \text{LR}_T$  are i.i.d. under  $\mathbf{H}_0$ .  $\square$

### E.2. Proof of Corollary E.2

**Corollary E.2** (SeMI<sup>max</sup> Type I Error). *The Type I error of SeMI<sup>max</sup> with threshold  $\gamma$  is*

$$\alpha_{\max}(\gamma) = 1 - [1 - \alpha_0(\gamma)]^T$$

where  $\alpha_0(\gamma)$  is the Type I error of the single-batch test from Lemma 3.5.

*Proof.* The SeMI<sup>max</sup> test rejects when  $\max_{\tau=1, \dots, T} \log \text{LR}_\tau \geq \gamma$ . The Type I error is:

$$\begin{aligned} \alpha_{\max}(\gamma) &= P_0(\text{SeMI}^{\max} \geq \gamma) \\ &= P_0\left(\max_{\tau=1, \dots, T} \log \text{LR}_\tau \geq \gamma\right) \\ &= 1 - P_0(\log \text{LR}_\tau < \gamma \text{ for all } \tau). \end{aligned}$$

By Theorem E.1, the statistics are independent under  $\mathbf{H}_0$ :

$$P_0(\log \text{LR}_\tau < \gamma \text{ for all } \tau) = \prod_{\tau=1}^T P_0(\log \text{LR}_\tau < \gamma).$$

Since all  $\log \text{LR}_\tau$  have the same distribution under  $\mathbf{H}_0$ :

$$\prod_{\tau=1}^T P_0(\log \text{LR}_\tau < \gamma) = [P_0(\log \text{LR}_1 < \gamma)]^T = [1 - \alpha_0(\gamma)]^T.$$

Therefore:

$$\alpha_{\max}(\gamma) = 1 - [1 - \alpha_0(\gamma)]^T.$$

$\square$

To achieve overall Type I error  $\alpha$ , set the threshold  $\gamma^*$  such that  $\alpha_0(\gamma^*) = 1 - (1 - \alpha)^{1/T}$ . For small  $\alpha$  and moderate  $T$ , this approximates the Bonferroni correction  $\alpha_0 \approx \alpha/T$ .

### E.3. Proof of Corollary E.3

**Corollary E.3** (SeMI<sup>max</sup> Type II Error). *The Type II error of SeMI<sup>max</sup>, given true insertion time  $\tau^*$ , is*

$$\beta_{\max}(\gamma \mid \tau^*) = \beta_0(\gamma) \cdot [1 - \alpha_0(\gamma)]^{T-1}$$

where  $\beta_0(\gamma)$  is the Type II error from Lemma 3.6. This does not depend on  $\tau^*$ .

*Proof.* Under  $\mathbf{H}_1^{\tau^*}$ , the target  $z^*$  is in batch  $\tau^*$ . The Type II error is the probability of failing to reject  $\mathbf{H}_0$ .

The test fails to reject when all log likelihood ratios are below the threshold:

$$\beta_{\max}(\gamma | \tau^*) = P_1(\text{SeMI}^{\max} < \gamma | \mathbf{H}_1^{\tau^*}) = P_1\left(\max_{\tau} \log \text{LR}_{\tau} < \gamma\right).$$

Separating the true insertion time from others:

$$P_1\left(\max_{\tau} \log \text{LR}_{\tau} < \gamma\right) = P_1\left(\log \text{LR}_{\tau^*} < \gamma \text{ and } \max_{\tau \neq \tau^*} \log \text{LR}_{\tau} < \gamma\right).$$

Under  $\mathbf{H}_1^{\tau^*}$ , the statistic  $\log \text{LR}_{\tau^*}$  depends only on batch  $D_{\tau^*}$ , while  $\log \text{LR}_{\tau}$  for  $\tau \neq \tau^*$  depends only on batch  $D_{\tau}$ . Since the batches are independent, these statistics are independent:

$$P_1\left(\log \text{LR}_{\tau^*} < \gamma \text{ and } \max_{\tau \neq \tau^*} \log \text{LR}_{\tau} < \gamma\right) = P_1(\log \text{LR}_{\tau^*} < \gamma) \cdot P_1\left(\max_{\tau \neq \tau^*} \log \text{LR}_{\tau} < \gamma\right).$$

The first factor is  $\beta_0(\gamma)$ , the Type II error of the single-batch test. For batches  $\tau \neq \tau^*$ , no target is present, so  $\log \text{LR}_{\tau}$  has the null distribution. By the same argument as in Corollary E.2:

$$P_1\left(\max_{\tau \neq \tau^*} \log \text{LR}_{\tau} < \gamma\right) = [1 - \alpha_0(\gamma)]^{T-1}.$$

Therefore:

$$\beta_{\max}(\gamma | \tau^*) = \beta_0(\gamma) \cdot [1 - \alpha_0(\gamma)]^{T-1}.$$

The result does not depend on  $\tau^*$  because both  $\alpha_0(\gamma)$  and  $\beta_0(\gamma)$  are independent of the insertion time.  $\square$

The Type II error decomposes as a product:  $\beta_0(\gamma)$  is the probability that the test fails to detect the target in the correct batch, and  $[1 - \alpha_0(\gamma)]^{T-1}$  is the probability that none of the other batches trigger a false detection. Independence from  $\tau^*$  follows from the identical distribution of batch means.

## F. SGD Analysis

We consider the SGD setting where we observe model parameters  $\theta_0, \theta_1, \dots, \theta_T$  with  $\theta_t \in \mathbb{R}^d$ . At each step  $t$ , the update is  $\theta_t = \theta_{t-1} - \eta_t g_t$  where  $\eta_t > 0$  is the learning rate and  $g_t$  is the batch gradient on dataset  $D_t$  of size  $n_t$ . The target  $z^*$  lies in the data domain  $\mathcal{X}$  and the insertion time  $\tau$  is known. We test:

$$\begin{aligned} \mathbf{H}_0 &: \text{All samples in } D_1, \dots, D_T \text{ are drawn i.i.d. from } \mathcal{D} \\ \mathbf{H}_1^{\tau} &: \text{One sample in } D_{\tau} \text{ is replaced by } z^* \end{aligned}$$

We assume that, conditioned on  $\theta_{t-1}$ , the batch gradient  $g_t$  is Gaussian with mean  $\mu_g(\theta_{t-1})$  and covariance  $\Sigma_g(\theta_{t-1})/n_t$ . This approximation is justified by the central limit theorem when the batch aggregates gradients from many data points.

**Notation.** The loss function on data point  $x$  with parameter  $\theta$  is denoted by  $\ell(\theta; x)$ . The batch gradient is  $g_t = \frac{1}{n_t} \sum_{x \in D_t} \nabla_{\theta} \ell(\theta_{t-1}; x)$ . We denote by  $\mu_g(\theta)$  and  $\Sigma_g(\theta)$  the mean and covariance of the batch gradient when scaled by  $\sqrt{n_t}$ , i.e.,  $g_t | \theta_{t-1} \sim \mathcal{N}(\mu_g(\theta_{t-1}), \Sigma_g(\theta_{t-1})/n_t)$ .

### F.1. Conditional Distributions

**Lemma F.1** (Parameter Distribution Under  $\mathbf{H}_0$ ). *Under  $\mathbf{H}_0$ , the conditional distribution of  $\theta_t$  given  $\theta_{t-1}$  is:*

$$\theta_t | \theta_{t-1}, \mathbf{H}_0 \sim \mathcal{N}\left(\theta_{t-1} - \eta_t \mu_g(\theta_{t-1}), \frac{\eta_t^2 \Sigma_g(\theta_{t-1})}{n_t}\right).$$

**Lemma F.2** (Parameter Distribution Under  $\mathbf{H}_1^\tau$ ). *Under  $\mathbf{H}_1^\tau$ , the conditional distribution of  $\theta_\tau$  given  $\theta_{\tau-1}$  is:*

$$\theta_\tau \mid \theta_{\tau-1}, \mathbf{H}_1^\tau \sim \mathcal{N} \left( \theta_{\tau-1} - \eta_\tau \cdot \frac{(n_\tau - 1)\mu_g(\theta_{\tau-1}) + \nabla_\theta \ell(\theta_{\tau-1}; z^*)}{n_\tau}, \frac{\eta_\tau^2(n_\tau - 1)\Sigma_g(\theta_{\tau-1})}{n_\tau^2} \right).$$

For  $t \neq \tau$ , the conditional distribution is identical to that under  $\mathbf{H}_0$ .

*Proof.* **Batch gradient under  $\mathbf{H}_1^\tau$ .** Batch  $D_\tau$  contains  $(n_\tau - 1)$  samples from  $\mathcal{D}$  and the fixed target  $z^*$ . The batch gradient is:

$$g_\tau = \frac{1}{n_\tau} \left[ \sum_{i=1}^{n_\tau-1} \nabla_\theta \ell(\theta_{\tau-1}; x_i) + \nabla_\theta \ell(\theta_{\tau-1}; z^*) \right].$$

Under the Gaussian gradient assumption, the sum of  $(n_\tau - 1)$  i.i.d. Gaussian gradients has mean  $(n_\tau - 1)\mu_g(\theta_{\tau-1})$  and covariance  $(n_\tau - 1)\Sigma_g(\theta_{\tau-1})$ . Adding the fixed target gradient shifts the mean.

The result follows from  $\theta_\tau = \theta_{\tau-1} - \eta_\tau g_\tau$ .  $\square$

## F.2. Likelihood Ratio

**Theorem F.3** (SGD Likelihood Ratio Simplification). *The likelihood ratio for testing  $\mathbf{H}_0$  against  $\mathbf{H}_1^\tau$  based on  $(\theta_0, \dots, \theta_T)$  satisfies:*

$$\frac{p(\theta_0, \dots, \theta_T \mid \mathbf{H}_1^\tau)}{p(\theta_0, \dots, \theta_T \mid \mathbf{H}_0)} = \frac{p(\theta_\tau \mid \theta_{\tau-1}, \mathbf{H}_1^\tau)}{p(\theta_\tau \mid \theta_{\tau-1}, \mathbf{H}_0)}.$$

*Proof.* By the chain rule,

$$\frac{p(\theta_0, \dots, \theta_T \mid H)}{p(\theta_0)} = \prod_{t=1}^T p(\theta_t \mid \theta_0, \dots, \theta_{t-1}, H).$$

The update  $\theta_t = \theta_{t-1} - \eta_t g_t$  implies that  $\theta_t$  depends on  $(\theta_0, \dots, \theta_{t-1})$  only through  $\theta_{t-1}$ , since  $g_t$  depends on  $\theta_{t-1}$  and the samples in  $D_t$ . Thus

$$p(\theta_t \mid \theta_0, \dots, \theta_{t-1}, H) = p(\theta_t \mid \theta_{t-1}, H).$$

The likelihood ratio becomes

$$\text{LR} = \prod_{t=1}^T \frac{p(\theta_t \mid \theta_{t-1}, \mathbf{H}_1^\tau)}{p(\theta_t \mid \theta_{t-1}, \mathbf{H}_0)}.$$

For  $t < \tau$ , the target has not been inserted, so both conditional distributions are identical and the ratio equals 1. For  $t > \tau$ , batch  $D_t$  contains no target under either hypothesis, so conditioned on  $\theta_{t-1}$  the distributions coincide and the ratio equals 1. Only the term at  $t = \tau$  contributes.  $\square$

**Theorem F.4** (SGD Log Likelihood Ratio). *Define  $\delta_g = \nabla_\theta \ell(\theta_{\tau-1}; z^*) - \mu_g(\theta_{\tau-1})$  and  $N = \theta_\tau - \theta_{\tau-1} + \eta_\tau \mu_g(\theta_{\tau-1})$ . The log likelihood ratio is:*

$$\begin{aligned} \log \text{LR} &= -\frac{d}{2} \log \left( \frac{n_\tau - 1}{n_\tau} \right) - \frac{n_\tau}{2(n_\tau - 1)\eta_\tau^2} N^\top \Sigma_g^{-1} N \\ &\quad - \frac{n_\tau}{(n_\tau - 1)\eta_\tau} N^\top \Sigma_g^{-1} \delta_g - \frac{m^*}{2(n_\tau - 1)} \end{aligned}$$

where  $m^* = \delta_g^\top \Sigma_g^{-1} \delta_g$  is the Mahalanobis distance of the target gradient from the population mean. We denote this sequential test for SGD as SeMI<sup>SGD</sup>.

*Proof.* **Conditional parameters.** Let  $m_0 = \theta_{\tau-1} - \eta_\tau \mu_g(\theta_{\tau-1})$  and  $m_1 = \theta_{\tau-1} - \eta_\tau \frac{(n_\tau - 1)\mu_g(\theta_{\tau-1}) + \nabla_\theta \ell(\theta_{\tau-1}; z^*)}{n_\tau}$ . The covariances are  $V_0 = \frac{\eta_\tau^2 \Sigma_g}{n_\tau}$  and  $V_1 = \frac{\eta_\tau^2 (n_\tau - 1) \Sigma_g}{n_\tau^2}$ .

**Mean difference.**

$$m_1 - m_0 = -\frac{\eta_\tau}{n_\tau} (\nabla_\theta \ell(\theta_{\tau-1}; z^*) - \mu_g(\theta_{\tau-1})) = -\frac{\eta_\tau \delta_g}{n_\tau}.$$

**Log likelihood ratio.** With  $N = \theta_\tau - m_0$ , expand the quadratic terms and substitute  $V_0^{-1} = \frac{n_\tau}{\eta_\tau^2} \Sigma_g^{-1}$ . Collecting terms yields the stated result.  $\square$

**Theorem F.5** (Distribution of the Log Likelihood Ratio). *Under  $\mathbf{H}_0$ :*

$$N \mid \theta_{\tau-1}, \mathbf{H}_0 \sim \mathcal{N} \left( 0, \frac{\eta_\tau^2 \Sigma_g}{n_\tau} \right).$$

*Under  $\mathbf{H}_1^\tau$ :*

$$N \mid \theta_{\tau-1}, \mathbf{H}_1^\tau \sim \mathcal{N} \left( -\frac{\eta_\tau \delta_g}{n_\tau}, \frac{\eta_\tau^2 (n_\tau - 1) \Sigma_g}{n_\tau^2} \right).$$

*Proof.* Under  $\mathbf{H}_0$ ,  $\theta_\tau \mid \theta_{\tau-1} \sim \mathcal{N}(m_0, V_0)$  with  $m_0 = \theta_{\tau-1} - \eta_\tau \mu_g(\theta_{\tau-1})$ . Since  $N = \theta_\tau - m_0$ , we have  $N \sim \mathcal{N}(0, V_0)$ .

Under  $\mathbf{H}_1^\tau$ ,  $\theta_\tau \mid \theta_{\tau-1} \sim \mathcal{N}(m_1, V_1)$ . Thus  $N = \theta_\tau - m_0 \sim \mathcal{N}(m_1 - m_0, V_1)$ . Recalling that  $m_1 - m_0 = -\frac{\eta_\tau \delta_g}{n_\tau}$ , we have the stated mean and covariance.  $\square$

### F.3. Application to Linear Regression

For linear regression with squared loss  $\ell(\theta; (x, y)) = \frac{1}{2}(y - \theta^\top x)^2$  and Gaussian covariates  $x \sim \mathcal{N}(0, \Sigma_x)$ :

**Lemma F.6** (Mean Gradient). *Let  $\Delta = \theta - \theta^*$ . The mean gradient is  $\mu_g(\theta) = \Sigma_x \Delta$ .*

*Proof.* Let  $\nabla_\theta \ell(\theta; (x, y)) = (\theta^\top x - y)x = (\theta^\top x - \theta^{*\top} x - \varepsilon)x = (\Delta^\top x - \varepsilon)x$ . Taking expectations:

$$\mu_g(\theta) = \mathbb{E}[(\Delta^\top x)x] - \mathbb{E}[\varepsilon]\mathbb{E}[x] = \mathbb{E}[xx^\top]\Delta = \Sigma_x \Delta.$$

$\square$

**Lemma F.7** (Gradient Covariance). *The covariance of the per-sample gradient is:*

$$\Sigma_g(\theta) = (\sigma_\varepsilon^2 + \Delta^\top \Sigma_x \Delta)\Sigma_x + \Sigma_x \Delta \Delta^\top \Sigma_x.$$

*Proof.* The second moment is  $\mathbb{E}[gg^\top] = \mathbb{E}[(\Delta^\top x - \varepsilon)^2 xx^\top]$ . Since  $\varepsilon \perp x$  and  $\mathbb{E}[\varepsilon] = 0$ :

$$\mathbb{E}[gg^\top] = \mathbb{E}[(\Delta^\top x)^2 xx^\top] + \sigma_\varepsilon^2 \Sigma_x.$$

Using Isserlis' theorem for the fourth moment of Gaussian  $x$ :

$$\mathbb{E}[(\Delta^\top x)^2 xx^\top] = (\Delta^\top \Sigma_x \Delta)\Sigma_x + 2\Sigma_x \Delta \Delta^\top \Sigma_x.$$

The covariance is  $\Sigma_g = \mathbb{E}[gg^\top] - \mu_g \mu_g^\top$ . Subtracting  $\mu_g \mu_g^\top = \Sigma_x \Delta \Delta^\top \Sigma_x$  yields the result.  $\square$

**Corollary F.8** (Gradient Statistics at Optimum). *At  $\theta = \theta^*$ , we have  $\Delta = 0$ , so  $\mu_g(\theta^*) = 0$  and  $\Sigma_g(\theta^*) = \sigma_\varepsilon^2 \Sigma_x$ .*

**Lemma F.9** (Target Gradient Deviation). *At  $\theta = \theta^*$ , the target gradient is  $\nabla_\theta \ell(\theta^*; (x^*, y^*)) = -\varepsilon^* x^*$  where  $\varepsilon^*$  is the target residual. The deviation from the population mean is  $\delta_g = -\varepsilon^* x^*$ .*

*Proof.* At optimum,  $\nabla_\theta \ell = (\theta^{*\top} x^* - y^*)x^* = -\varepsilon^* x^*$ . Since  $\mu_g(\theta^*) = 0$ ,  $\delta_g = -\varepsilon^* x^*$ .  $\square$

**Theorem F.10** (Detectability at Optimum). *At  $\theta = \theta^*$ , the Mahalanobis distance of the target gradient is:*

$$m^* = \frac{(\varepsilon^*)^2}{\sigma_\varepsilon^2} \cdot (x^*)^\top \Sigma_x^{-1} x^*.$$

*This factors as product of a label outlier score  $(\varepsilon^*/\sigma_\varepsilon)^2$  and a feature leverage score  $(x^*)^\top \Sigma_x^{-1} x^*$ .*

*Proof.* Substituting into  $m^* = \delta_g^\top \Sigma_g(\theta^*)^{-1} \delta_g$ :

$$m^* = (-\varepsilon^* x^*)^\top (\sigma_\varepsilon^2 \Sigma_x)^{-1} (-\varepsilon^* x^*) = \frac{(\varepsilon^*)^2}{\sigma_\varepsilon^2} (x^*)^\top \Sigma_x^{-1} x^*.$$

□

Samples with large residuals (relative to population noise) and unusual feature vectors (relative to population covariance) are most detectable.

## G. Proof of Auditing

**Lemma 5.1.** *If the mechanism used in SeMI satisfies  $(\varepsilon, \delta)$ -DP, then  $\mathbb{P}(\varepsilon \geq \varepsilon_R^\xi(\delta)) \geq 1 - \xi$ .*

*Proof.* The  $N_1(R)$  values of  $T_i$  such that  $B_i = 1$  are i.i.d.  $\beta(\gamma)$  can be interpreted as the cdf of  $T_i | B_i = 1$ . Using the DKW inequality (Massart, 1990), which provides a uniform concentration of the empirical cdf ( $\widehat{\beta}_R(\gamma)$ ), we have

$$\mathbb{P}\left(\sup_\gamma |\widehat{\beta}_R(\gamma) - \beta(\gamma)| > \sqrt{\frac{\log(\xi/4)}{2N_1(R)}}\right) \leq \xi/2$$

Using a similar argument for  $\alpha$  and a union bound yields

$$\mathbb{P}\left(\forall \gamma \in \mathbb{R}, \alpha(\gamma) \leq \overline{\alpha}_R^\xi(\gamma), \beta(\gamma) \leq \overline{\beta}_R^\xi(\gamma)\right) \geq 1 - \xi$$

The conclusion follows from Inequality (2). □

## H. Additional Experiments

This appendix provides additional experimental results supporting the main paper. We examine the GLR test for unknown insertion time, validation on SGD, sensitivity to unknown parameters, and the multivariate setting.

### H.1. Unknown Insertion Time

This section provides additional results for the sequential tests when the insertion time  $\tau$  is unknown. We use  $n = 10$ ,  $\mu = 0$ ,  $\sigma = 1$ , and target  $z^*$  with Mahalanobis distance 3. Power comparisons as a function of  $T$  and signal strength appear in the main text (Figure 2).

Figure 4 shows ROC curves for different values of  $T$ . As  $T$  increases, the gap between SeMI\* and the other methods widens, while SeMI<sup>Unif</sup> and SeMI<sup>max</sup> maintain an advantage over Final Observation.

**Uniformly Sampled  $\tau$ .** The preceding experiments fix the insertion time  $\tau$  and evaluate the GLR test that maximizes over candidate values. We now consider the composite hypothesis setting where the insertion time is itself random: under  $\mathbf{H}_1$ , the target  $z^*$  is inserted at  $\tau \sim \text{Uniform}(1, T)$ . This formulation captures scenarios where the auditor has no prior knowledge about when a datapoint might have been added.

Figure 5 shows ROC curves and power as a function of signal strength. The qualitative behavior matches the fixed- $\tau$  case: SeMI<sup>max</sup> outperforms the Final Observation baseline at large Mahalanobis distances, while SeMI\* (which knows the true  $\tau$ ) provides an upper bound.

Figure 6 displays power versus  $T$ . The gap between SeMI\* and SeMI<sup>max</sup> persists, confirming that estimating the insertion time introduces a cost even when  $\tau$  is uniformly distributed.

### H.2. SGD Validation

We validate the extension to SGD (Section 4) using linear regression with  $d = 5$  features,  $T = 10$  updates, batch size  $n = 50$ , and learning rate  $\eta = 0.05$ .

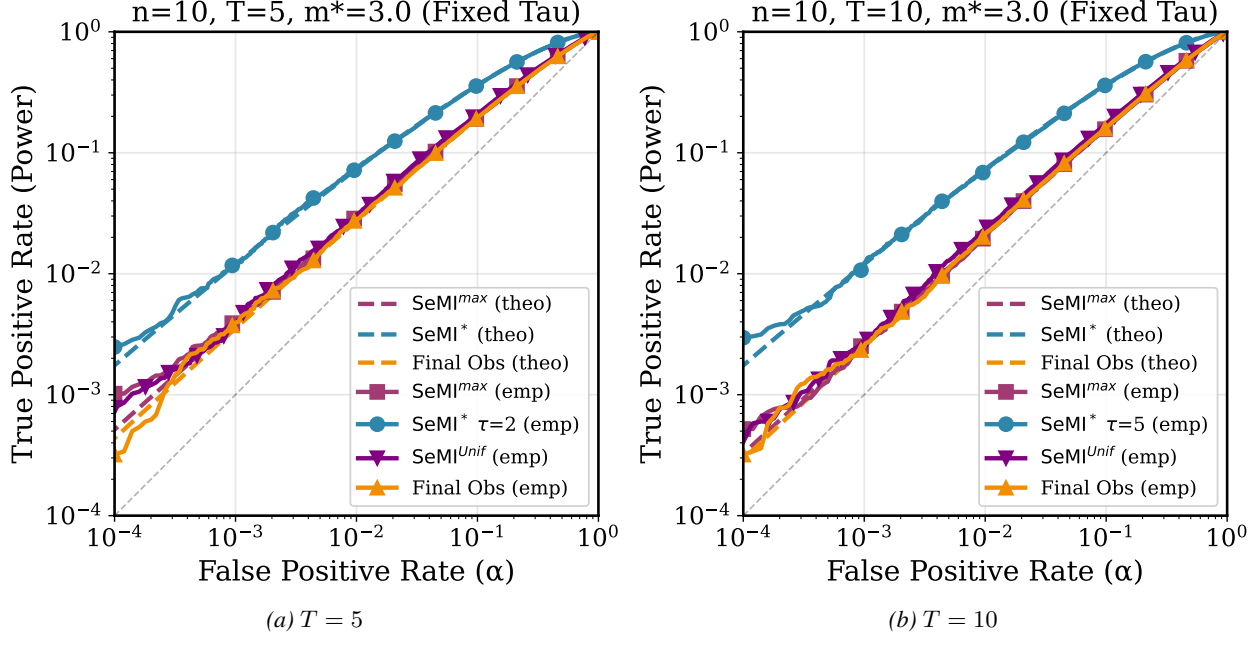


Figure 4. ROC curves comparing  $\text{SeMI}^*$ ,  $\text{SeMI}^{\text{Unif}}$ ,  $\text{SeMI}^{\text{max}}$ , and Final Observation for different  $T$ .

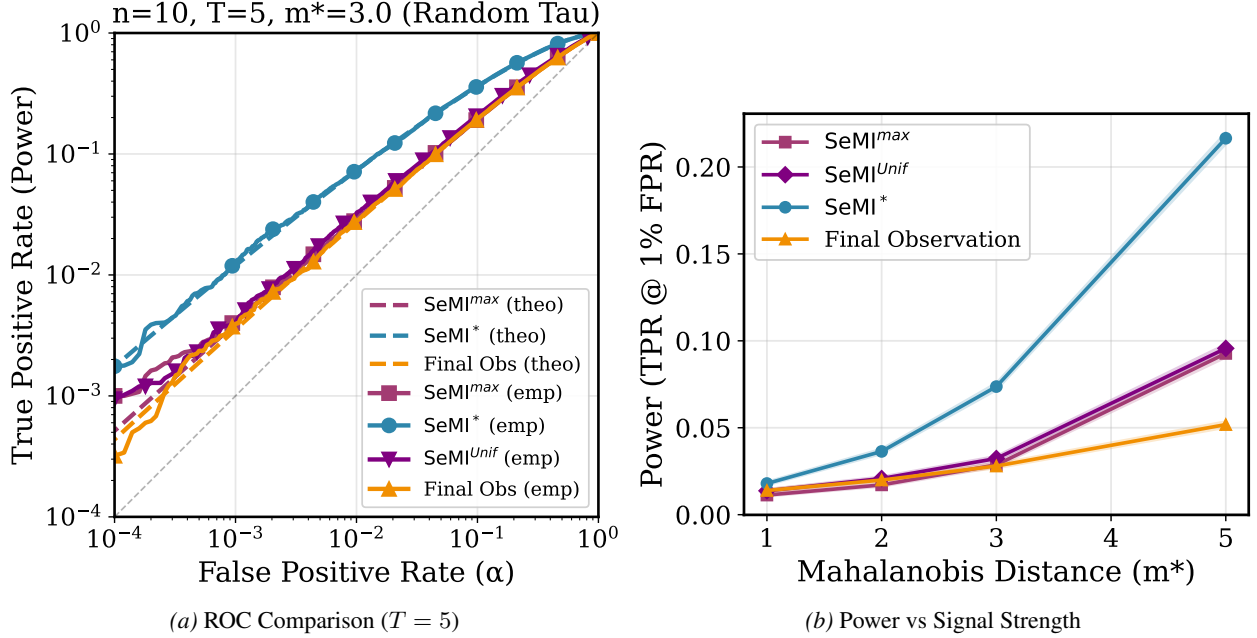


Figure 5. Composite hypothesis setting with  $\tau \sim \text{Uniform}(1, T)$ . (a) ROC curves comparing  $\text{SeMI}^{\text{max}}$ ,  $\text{SeMI}^*$ , and Final Observation. (b) Power vs Mahalanobis distance.

Figure 7(a) shows ROC curves for insertion at  $\tau = 5$ .  $\text{SeMI}^{\text{SGD}}$  outperforms the Delta and Back-Front heuristics from Jagielski et al. (2023).

Figure 7(b) shows power as a function of insertion time  $\tau$ . The Back-Front statistic maintains constant power with respect to  $\tau$  because it depends only on endpoints and gradient effects persist in convex landscapes. The Delta statistic shows decreasing power as  $\tau$  increases: early in training, gradient magnitudes are larger, producing stronger signals.  $\text{SeMI}^{\text{SGD}}$  maintains high power across all  $\tau$ .

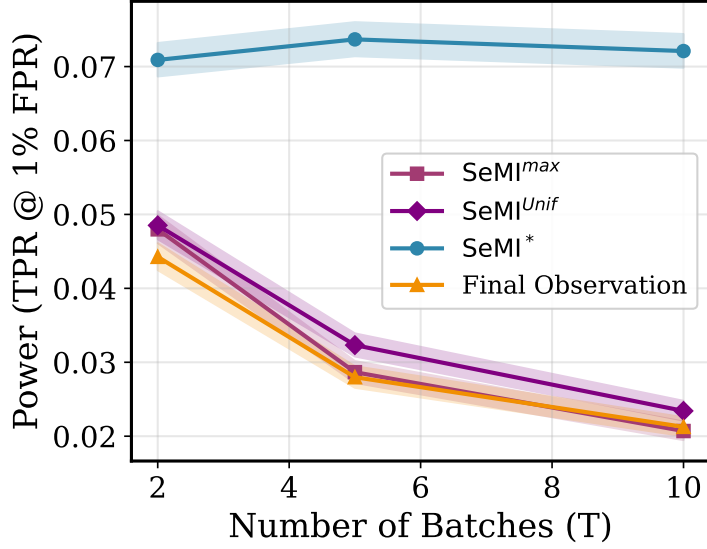


Figure 6. Power vs  $T$  under composite hypothesis ( $\tau \sim \text{Uniform}(1, T)$ ). The gap between oracle and GLR persists.

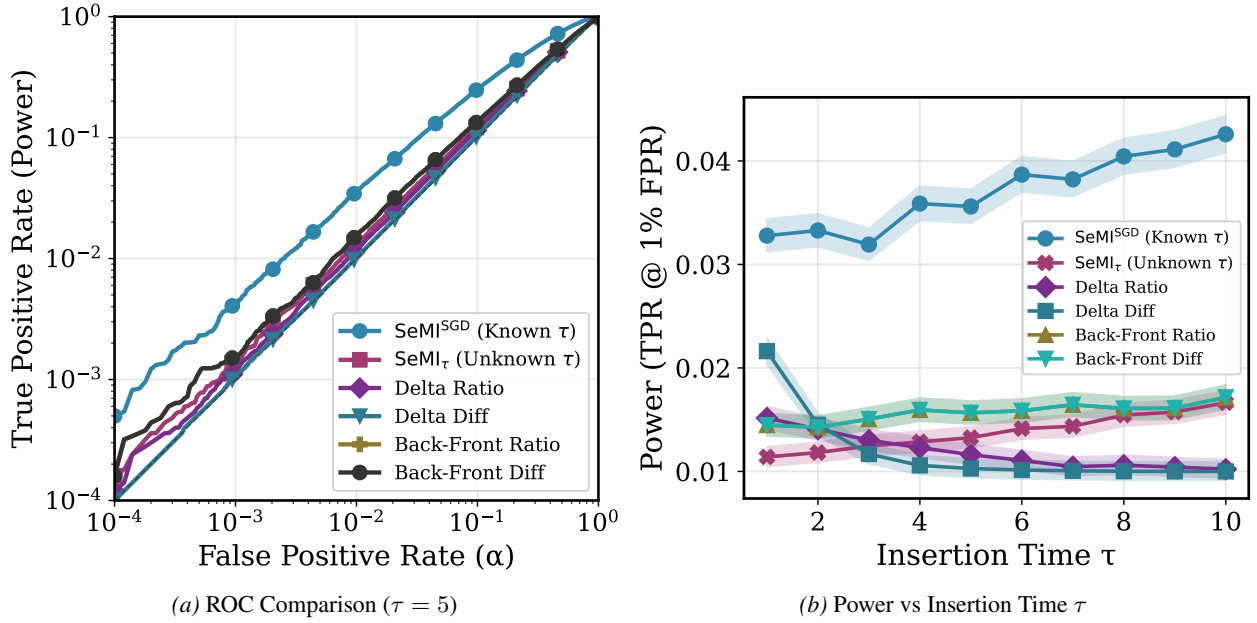


Figure 7. SGD validation on linear regression. (a) ROC curves. (b) Power vs  $\tau$ .  $\text{SeMI}^{\text{SGD}}$  maintains power regardless of insertion time.

### H.3. Multivariate Setting

We test the extension to  $d$ -dimensional Gaussian data (Appendix B). Parameters:  $n = 10$ ,  $T = 5$ ,  $\tau = 3$ , target  $z^*$  with Mahalanobis distance 3 from the mean.

Figure 8(a) displays the decision boundary in  $d = 2$ . Figure 8(b) shows that power remains constant as dimension  $d$  increases from 2 to 50. For a fixed Mahalanobis distance, the test statistic depends on the projection onto the target direction, making power independent of ambient dimension.

### H.4. DP-SGD Fine-tuning: ROC Curves

This section provides ROC curves for the privacy auditing experiments on DP-SGD fine-tuning (Section 5). We show results for Fashion-MNIST at two privacy levels: non-private ( $\varepsilon = \infty$ ) and private ( $\varepsilon = 1.0$ ).

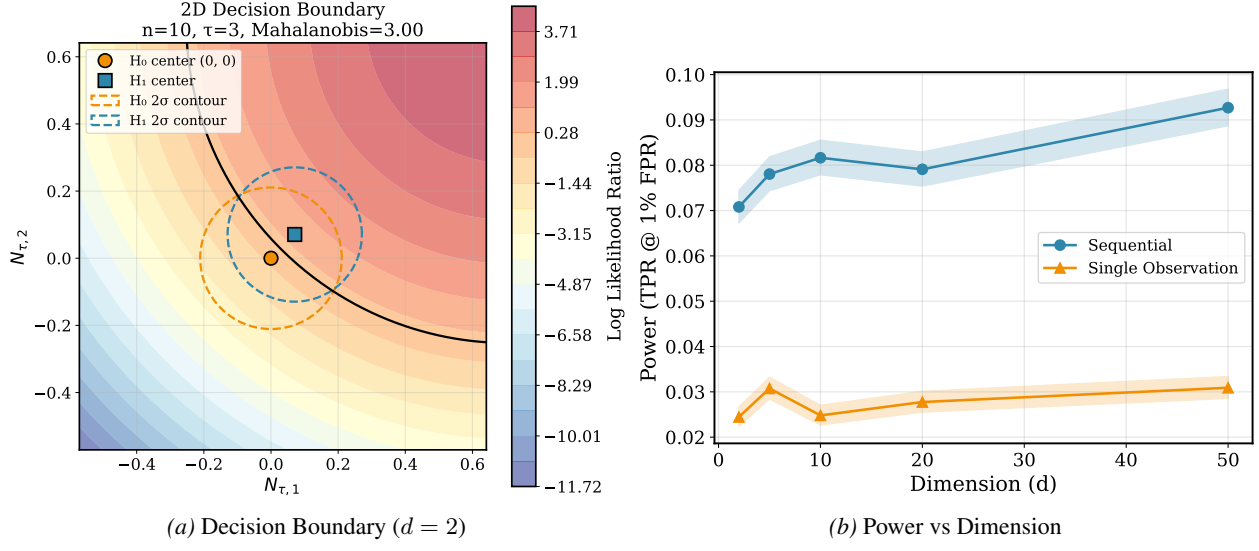


Figure 8. Multivariate setting. (a) Decision boundary in 2D. (b) Power vs dimension  $d$ .

Figure 9(a) shows the non-private setting.  $\text{SeMI}^{\text{SGD}}$  and  $\text{SeMI}^{\text{max}}$  both achieve near-perfect discrimination (AUC  $\approx 1.0$ ), while the heuristic baselines perform substantially worse (Back-Front AUC  $\approx 0.80$ , Delta AUC  $\approx 0.65$ ). This confirms that the likelihood ratio test exploits gradient information more effectively than loss-based heuristics.

Figure 9(b) shows the private setting ( $\varepsilon = 1.0$ ). All methods degrade due to the DP noise, but  $\text{SeMI}^{\text{SGD}}$  maintains an advantage (AUC = 0.60) over baselines (AUC  $\approx 0.51$ –0.53). The gap is most pronounced at low false positive rates, which are relevant for privacy auditing where conservative bounds are desired.

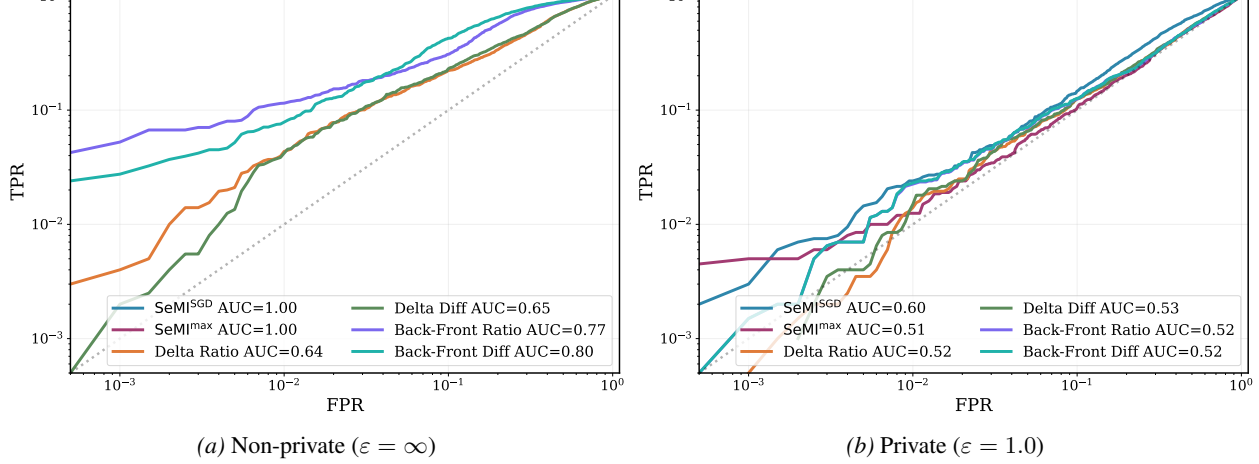


Figure 9. ROC curves for Fashion-MNIST fine-tuning. (a) Without DP noise,  $\text{SeMI}^{\text{SGD}}$  achieves near-perfect discrimination. (b) With DP-SGD ( $\varepsilon = 1.0$ ),  $\text{SeMI}^{\text{SGD}}$  maintains an advantage over heuristic baselines.

## H.5. Effect of Insertion Time Selection

The main text reports privacy lower bounds averaged over insertion times  $\tau \in \{1, \dots, T\}$ . Here we compare this averaging strategy against selecting the best  $\tau$  post hoc, i.e., reporting the tightest bound across all insertion times.

Figure 10 shows results for Fashion-MNIST. Solid lines show the averaged estimates; dashed lines show the maximum (best  $\tau$ ) estimates. For  $\text{SeMI}^{\text{SGD}}$ , selecting the best  $\tau$  yields substantially tighter bounds, particularly at moderate privacy levels ( $\varepsilon \in [0.5, 2]$ ). The gap between Average and Max indicates that some insertion times are more favorable for auditing than others.

This observation suggests that an auditor who can choose when to insert the target, or who audits at multiple insertion times and reports the best result, can obtain tighter privacy lower bounds. Determining which  $\tau$  is optimal a priori for a given architecture and dataset remains an open question for future work.

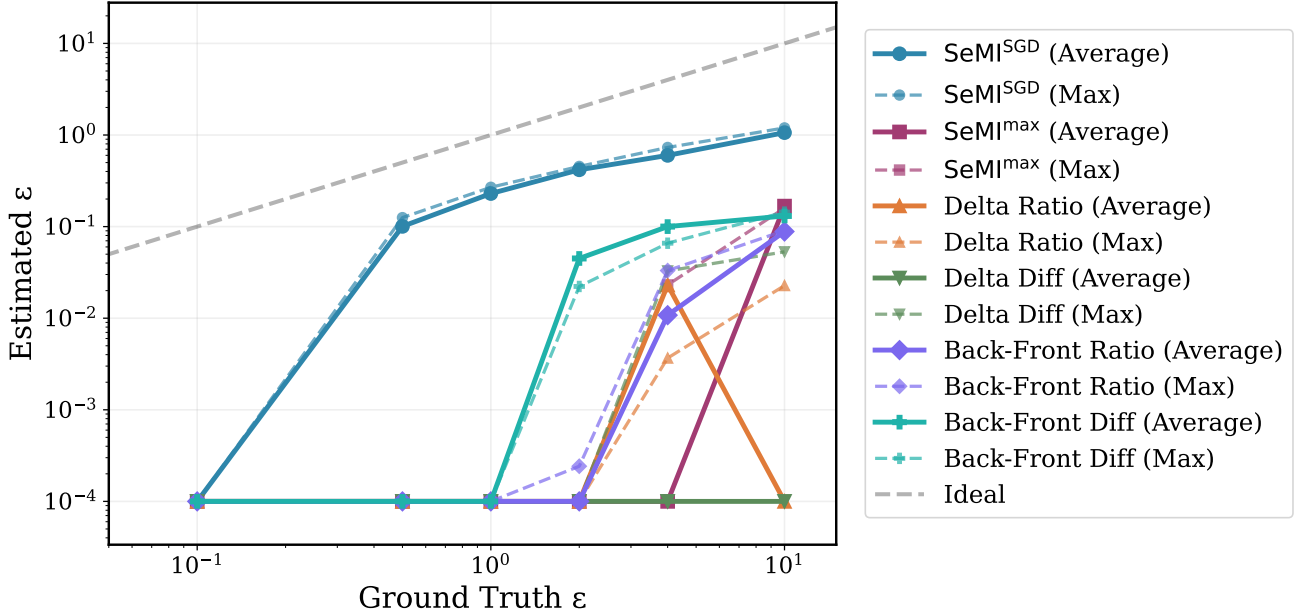


Figure 10. Effect of insertion time selection on Fashion-MNIST. Solid lines: averaged over  $\tau$ . Dashed lines: best  $\tau$  (post hoc selection). Selecting the optimal insertion time yields tighter privacy lower bounds.